Vol 3
Dec 2017

PMUSER

Proceedings of Manitoba's Undergraduate Science and Engineering Research

Frontiers of Undergraduate Research

Table of Contents

About the Cover

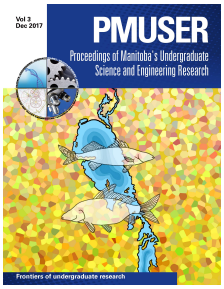

The cover image was designed by Chloé Schmidt to recognize the recipient of the 'Best Paper Award'. Sarah Warrack's paper, *Microplastics Flowing into Lake Winnipeg: Densities, Sources, Flux, and Fish Exposures*, reflects her work as part of her B.Sc. (Hons.) in the Faculty of Environment at the University of Manitoba. Chloé, in addition to being a Ph.D. student in Biological Sciences, illustrates the findings of scientific papers from ecology and evolution on her blog Pineapples and Whales.

Proceedings of Manitoba's Undergraduate Science and Engineering Research

About PMUSER

Proceedings of Manitoba's Undergraduate Science and Engineering Research (*PMUSER*) is an open-access refereed journal that is published annually and hosted by the University of Manitoba. The journal accepts research or review manuscripts written by undergraduate students from any science or engineering related faculty including, but not limited to, Engineering; Science; Human Ecology; Environment, Earth, and Resources; Agriculture and Food Sciences; Nursing; and Medicine. Upon submission, each manuscript undergoes a double blind peer-review process by two undergraduate/graduate students from a pool associated with the respective research area.

Aims & Scope

The focus of *PMUSER* is three fold. The circulation of a peer-reviewed undergraduate journal will provide a chance for students to receive recognition for their research in a wide range of scientific disciplines. The undertaking of writing a journal manuscript will further enhance the understanding of the significance of their respective projects in a broader context. This, in turn, will foster a tremendous growth in their intellectual development outside of the classroom setting, and serves as preparation for a career in research.

Available at:
http://ojs.lib.umanitoba.ca/index.php/pmuser/about/editorialPolicies#focusAndScope.

Copyright Info

For Authors
PMUSER is licensed under a Creative Commons Attribution-ShareAlike 4.0 International License (https://creativecommons.org/licenses/by-sa/4.0). The authors hold the copyright to published articles without restriction, and retain publishing rights.

For Readers
Author(s) grant readers access to published articles freely as long as the original authors and citation details are identified. The article and associated content are published under a Creative Commons Attribution-ShareAlike 4.0 International License (https://creativecommons.org/licenses/by-sa/4.0).

Open Access Policy

This journal provides immediate open access to its content on the principle that making research freely available to the public supports a greater global exchange of knowledge.

Available at:
http://ojs.lib.umanitoba.ca/index.php/pmuser/about/editorialPolicies#openAccessPolicy.

Publication Info

ISSN 2561-1127 (Print)
ISSN 2561-1135 (Online)
PMUSER publishes one volume per year and is published by the University of Manitoba Libraries, University of Manitoba, Winnipeg, MB, Canada, R3T 2N2.
Email: pmuser@umanitoba.ca

Instructions for Authors

Undergraduate authors are encouraged to submit research or review articles in any science or engineering discipline. Detailed instructions are available at http://ojs.lib.umanitoba.ca/index.php/pmuser/about/submissions#onlineSubmissions. Please adhere to these instructions in the preparation of manuscripts.

Journal Website

http://ojs.lib.umanitoba.ca/index.php/pmuser
Electronic edition available at: http://ojs.lib.umanitoba.ca/index.php/pmuser/issue.

Indexed In

PMUSER is indexed in Google Scholar.

Letter from the Editor-in-Chief

What makes a good research or review article? Almost universally, a component of the answer will be clear communication. But upon delving deeper it quickly becomes apparent that what clear scientific writing looks like depends on the audience reading it. *Proceedings of Manitoba's Undergraduate Science and Engineering Research* (PMUSER) has a broad audience: those interested in the work of Manitoba's undergraduate science and engineering students. The key to reaching this diverse audience is in providing a broad enough context for the article to be approachable, a task accomplished with a carefully structured 'Introduction'. Equally important is the 'Conclusion', providing a clear communication of the relevance of the research/review and a summarizing or emphasizing of its key findings. Clear communication adds fundamental value to a scientific manuscript, regardless of the volume, novelty, or indeed even success of the research or results obtained. A third aspect of clear communication in scientific writing is selecting and condensing what is often a great deal of data into a set of clear and concise figures and tables that best convey the research narrative.

Scientific communication, however, does not end with the preparation of the manuscript itself. It also extends through the review process, for both author and reviewer. The best manuscripts explain the research and its rationale well enough that the reviewers, those familiar with the particular field, are not left questioning the relevance, methods, or conclusions of the work. The reviewers themselves have a responsibility to the authors to ensure their remarks unambiguously address the shortcomings of the manuscript so as to ensure its improvement prior to publication. And lastly, in responding to the reviewers' comments, authors must provide a clear response to the editors as to which suggestions were incorporated and which, with justification, were not. These responses facilitate an honest back-and-forth between author, reviewer, and editor to ensure a transparent review process and ultimately a high quality publication.

The ability to communicate complex concepts clearly, and to constructively critique colleagues and receive such feedback, is not only a skill relevant to academia or research. It is also relevant much more broadly to any career, requiring critical reflection of ones' own work, and of others', for the purposes of learning and of improving the end product.

Therefore, with the goals of PMUSER in mind, goals of understanding research in a broader context and of fostering growth beyond the classroom, it is with excitement that a prize for 'Best Paper' is being awarded for the first time with the publication of this volume. Congratulations to Sarah Warrack! Her manuscript submission excelled in meeting the above criteria. J. Challis, a member of the editorial team, was a co-author of this submission, and therefore was excluded from all discussion, deliberation, and ultimately decisions around the award recipient. Formally, the award decision was made by two members of the PMUSER editorial team and two external colleagues who each independently reviewed the original manuscripts, the reviewer comments, and the authors' revised manuscripts with the accompanying response letters and provided recommendations.

As a journal, communication not only matters, it is our duty and our product. We have a responsibility to ensure that the manuscripts we publish are able to reflect the quality of research done by Manitoba's undergraduate students and that it is accessible to as many people as possible. Thus, we are proud to unveil a more polished and professional layout in this volume that has been two years in the making. Additionally, acquiring International Standard Serial Numbers (ISSN) for PMUSER and publishing Discrete Object Identifiers (DOIs) for every article are further steps in becoming fully open access. We continue to work on expanding awareness of PMUSER among everyone who may find it a valuable, informative, or rewarding experience to read, review, or submit research and review papers in our journal.

With these achievements of 2017, I look forward to reaching the broader authorship of Manitoba's science and engineering undergraduates with a diversity of research and review submissions for Volume 4! Stay tuned as we look to advance Manitoba's *Frontiers of Undergraduate Research*.

Thanks for reading,

Matthew J. D. Doering
PMUSER Editor-in-Chief

University of Manitoba Faculty Profiles

Dr. John Anderson

Professor, Computer Science, U of M

What opportunities do undergraduates have in your lab?

Our lab does work in autonomous intelligent systems, studying the principles of artificial intelligence through the construction of whole systems designed to function in a given domain. We do many of our implementations on humanoid robots and deal with issues like balancing and hand-eye coordination that are more complicated and interesting than simple wheeled robots. There are opportunities in all of these areas.

Why is research experience valuable for undergraduates?

More and more classes are bringing in examples of research, but you get only a limited perspective in a class. You tend to see an overview of a finished project or a work well in progress, and this is very different than experiencing the process yourself. You also tend to be surprised at how much you actually apply from all the classes you have taken, not just ones you enjoyed the most or those you think are core to your field. A lab is also a busy place, and you see the connections between your research and lots of other work, and that the research process is much broader than just any one project.

What value do undergraduates get from publishing?

While getting a publication is often on students' minds in terms of having an artifact come out of their work (or even just adding something to their CV), the process itself is not something most students arrive knowing much about. Not only does getting something ready for publication improve writing and communication in general, the detail-oriented work of properly documenting a project and describing it so that others can make use of it improves many other skills. Literature reviews themselves are also important – after doing a few you begin to see that sometimes your early description of a problem can change a great deal once you see and relate the work others have done.

What does it take to be successful in computer science?

Our field is hugely broad, and part of being successful is a willingness to see at least a little of all its pieces. A bigger issue though is being able to focus on computation rather than tools – the languages, systems, machines you use today will come and go; even being good at those in use is a fleeting talent. Being able to focus on the principles and adapt them to the problems (and tools) you see over time is important.

What advice would you give students in computer science?

Try to expose yourself to a broad range of experiences; never discount a particular area because it does not agree with you very much. You will find over time that they are all relevant.

Dr. Mark Hanson

Associate Professor, Environment & Geography, U of M

What opportunities do undergraduates have in your lab?

Any number! I'd love to have a student come to me with a study or project they'd like to pursue. I enjoy coming up with honours and summer research for students, but I'm just one person, and my ideas are maybe getting stale.

Why is research experience valuable for undergraduates?

The importance would be similar to any area I suspect; to get a sense of whether that type of inquiry is for you. If not, you find out easily and early and can keep looking. It is also an opportunity to shine if you are willing to put in the time and effort. When an undergraduate excels in the lab, it is noticed. The experience also opens the door to graduate school or, at the very least, letters of recommendation from someone that has had some real interactions with the student.

What value do undergraduates get from publishing their research or literature reviews?

Publishing is the mechanism by which the scientific and other communities share what they have discovered (or not found, which can be just as important). Otherwise, what we have learned is lost. It also reveals to the student both the power and flaws of peer review. Peer review and publishing exists because people will spend the time, and even put their reputations out there, to see new knowledge shared. Someone takes the time and energy to evaluate our work, and we have this conversation around the quality and value of our work that few people outside the process experience or understand. The student gets to see that they are part of a bigger whole.

What does it take to be successful in ecotoxicology?

The cynic in me says you take single, un-replicated studies and observations and instead of questioning the data, you proclaim to all who will listen that you have found the contaminant X that is responsible for environmental problem Y. Those days, I hope, are changing. It is becoming more and more about better studies, data openness, and collaborations between academics, government, and industry in order to tackle the challenges we face collectively.

What advice would you give students in ecotoxicology?

Ecotoxicology is truly inter- and multi-disciplinary. I can't stress enough the need to take a diverse range of courses in the sciences (and statistics!). Finally, design your studies to refute your hypotheses. This goes pretty much for everyone. Your goal in the end should not be to see an 'effect', but to help better understand and protect the environment.

DOI: 10.5203/pmuser.201730578

Microplastics Flowing into Lake Winnipeg: Densities, Sources, Flux, and Fish Exposures

Sarah Warrack[1], Jonathan K. Challis[2], Mark L. Hanson[1], Michael D. Rennie[3]

[1]Department of Environment and Geography, University of Manitoba, Winnipeg, Canada, R3T 2N2
[2]Department of Chemistry, University of Manitoba, Winnipeg, Canada, R3T 2N2
[3]Department of Biology, Lakehead University, Ontario, Canada, P7B 5E1

Corresponding Author: Sarah Warrack (umwarras@myumanitoba.ca)

Abstract

*Microplastics (plastic particles < 5.0 mm in diameter) have been detected in freshwater ecosystems worldwide. Recently, surface concentrations of microplastics in Lake Winnipeg, Manitoba were shown to be comparable to those observed in Lake Erie, Ontario despite large differences between the lakes in terms of population density and industrial activity. To better understand potential sources of microplastics into Lake Winnipeg, two inflowing tributaries (the Red and Assiniboine rivers) and the lake outflow (the Nelson River) were sampled for microplastics. To determine the role of wastewater treatment plants in contributing to microplastic pollution, microplastic densities upstream and downstream of wastewater treatment plants in the city of Winnipeg were compared. Finally, to determine the bioavailability of microplastics to fishes, we evaluated the presence of microplastics in the gastrointestinal tracts of two fish species, common carp (*Cyprinus carpio*), and sauger (*Sander canadensis*), collected from the Red River. Microplastics in the Red and Assiniboine rivers were comparable to those from Great Lake tributaries, but were elevated four to six times relative to concentrations observed in the Nelson River, suggesting significant losses to settling in Lake Winnipeg. On average, densities of microplastics downstream of wastewater treatment plants were elevated and a significant correlation was observed between standardized daily effluent discharge from Winnipeg and river flux of microplastics/m^2/s. On average, sauger were found to contain one microplastic particle and carp were found to contain seven microplastics within their gastrointestinal tracts. The number of particles ingested did not appear to affect body condition of fish collected in this study.*

Keywords: microplastics, plastic debris, rivers, freshwater contamination

1 Introduction

Globally, there is heavy reliance on the use of plastics in the manufacturing of consumer products (Romeo et al., 2015) and many plastics eventually reach our waterways (Klein et al., 2015). Microplastics are defined as small plastic particles less than 5.0 mm in diameter (Eerkes-Merando et al., 2015) which can enter the environment in one of two ways, either directly as microscopic-sized plastics such as microbeads in cosmetic products or scrubbers in cleaning products, or indirectly as larger plastic debris that continuously fragment and degrade into smaller particles (Browne et al., 2011; Arthur et al., 2010; Cole et al., 2014). These larger plastics fragment in the environment due to photolytic, mechanical, or biological degradation (Browne et al., 2007). Current global plastic production is estimated to be 300 million metric tonnes annually and is increasing by 20 million metric tonnes each year (Europe, 2015). By comparison to other forms of anthropogenic pollution (i.e. non-plastics), the degradation time of plastic is very slow, potentially hundreds of years (Europe, 2015).

Microplastic sources include consumer products (microbeads), manufacturing products (larger pellets), textiles (fibres), atmospheric fallout (dust particles), and larger plastics, which break down over time into smaller particles (Browne et al., 2011; Driedger et al., 2015; Dris et al., 2016). When clothing is washed, synthetic microplastic fibres shed, making their way into the sewage (Browne et al., 2011) that is then treated by wastewater treatment plants. Plastic particles not captured by wastewater treatment plants are eventually released, via effluent, into freshwater systems (Browne et al., 2011). Wastewater treatment plants are a point source of microplastics (Eerkes-Merando et al., 2015) as plastic particles are small enough to pass through the filtration process and thus have the potential to enter lakes, rivers, and streams (Browne et al., 2007).

The transportation and accumulation of microplastics are unique in river systems, as the unidirectional current is flowing downstream. Densities of microplastics in the Chicago River were greater in riparian zones than in bottom sediments (Driedger et al., 2015), as the high velocities of the river prevents plastic particles from settling. Proximity to wastewater treatment plants, water body size, depth, ship

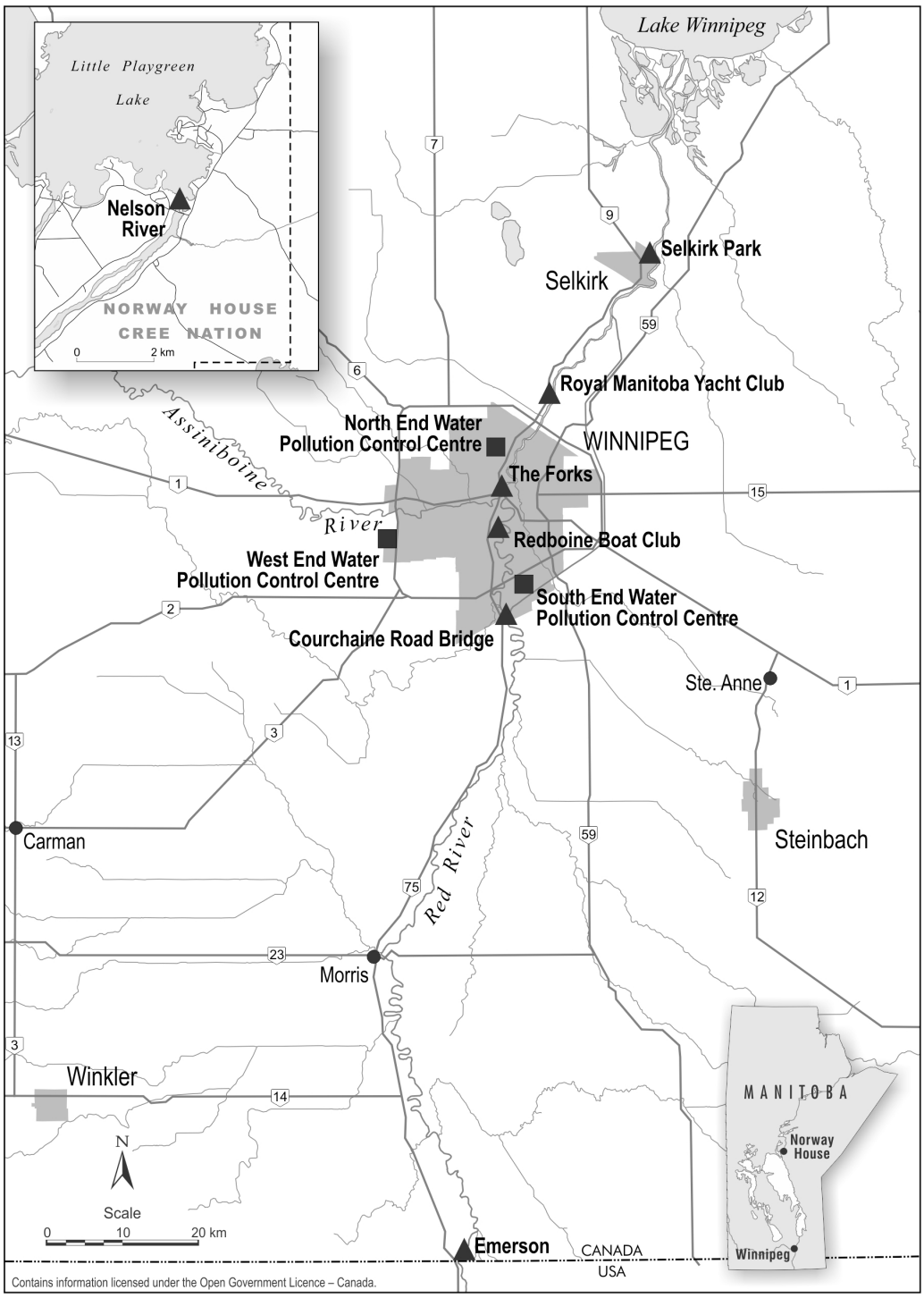

Figure 1: *Map of surface water and fish (Selkirk Park) sample collection sites (triangles) and Winnipeg's three wastewater treatment plants (squares): South End Water Pollution Control Centre (SEWPCC), North End Water Pollution Control Centre (NEWPCC), and West End Water Pollution Control Centre (WEWPCC). Emerson and Courchaine Road Bridge were upstream of SEWPCC. Redboine Boat Club downstream of SEWPCC. Royal Manitoba Yacht Club (RMYC) downstream of NEWPCC. The Forks site was downstream of WEWPCC.*

traffic, water turbulence events, seasonal events, water temperature, weather events, and geomorphological characteristics may all influence microplastic transport and possible accumulation of microplastics within a freshwater system (Mani et al., 2015; Fischer et al., 2016). Freshwater systems are likely a potential contributor to microplastic

loading in oceans (Eerkes-Merando et al., 2015). It is estimated that there are a minimum of five trillion plastic particles currently in the world's oceans, weighing approximately 250,000 tonnes (Eriksen et al., 2014).

Microplastics have been found inside the bodies of a wide variety of marine and freshwater organisms including invertebrates, fish, birds, and mammals (GESAMP, 2015), but the long-term impacts of microplastics on aquatic wildlife are not well understood (Masura et al., 2015). Microplastics may pose a possible hazard to human health through human consumption of aquatic species that contain plastic particles (Romeo et al., 2015), but there is no evidence of any human health impacts at this time.

Lake Winnipeg is the fifth largest Canadian lake and has the second largest watershed in Canada, over 982,000 km^2 (Anderson et al., 2017). The watershed is home to seven million people (20% of the Canadian population) and spans four Canadian provinces and four US states (Schindler, 2009). Lake Winnipeg has a greater density of microplastics per km^2 (193,420 $\pm$ 115,567 microplastics/ km^2) compared to Lake Superior (5,391 $\pm$ 4,552 microplastics/km^2) and Lake Huron (2,779 $\pm$ 2,440 microplastics/ km^2) (Anderson et al., 2017). By contrast, Lake Erie supports 12 million people in a watershed 1/10th the size of Lake Winnipeg (Anderson et al., 2017). The comparable densities between Lake Erie (105,503 $\pm$ 173,587 microplastics/ km^2) and Lake Winnipeg (193,420 $\pm$ 115,567 microplastics/ km^2) suggest that either long-range transport of microplastics from rivers is a major contributing source, or a potential source in the watershed may be missed with existing sampling campaigns (Anderson et al., 2017). The Red and Assiniboine rivers flow into Lake Winnipeg, and given their drainage through the city of Winnipeg likely contribute microplastics into the lake. The Nelson River drains Lake Winnipeg, and may be taking microplastics out of the lake. Understanding the potential inflow and outflow of microplastics in Lake Winnipeg by these three rivers provides important context for understanding the high densities observed in the lake (Anderson et al., 2017).

The purpose of this study was to collect and quantify microplastic densities in the surface waters of three Manitoban rivers, as well as to quantify fish ingestion of microplastics to establish a baseline for future monitoring. The data collected on the densities of microplastics in the inflow (Red and Assiniboine rivers) and outflow (Nelson River) of Lake Winnipeg will help to calculate microplastic loading in the lake. The study was also designed to investigate the potential influence that wastewater treatment plants may have on plastic densities in the rivers, as well as spatial and temporal trends. Specifically, we hypothesized that: (1) microplastic densities would be greatest downstream of wastewater treatment plants, and (2) microplastics would be ingested at higher numbers in benthic feeding species, where plastics are likely to be densest. The Assiniboine, Red, and Nelson rivers provide habitat for many fish and waterfowl species, and are culturally and economically important to Manitobans. Characterizing sources, ingestion by fish, and potential impacts of microplastics within the Assiniboine, Red, and Nelson rivers are important steps to further our understanding of this emerging environmental contaminant in freshwater systems.

2 Methods

2.1 Sampling Sites

Surface water from six study sites along the Assiniboine, Red, and Nelson rivers in Manitoba, Canada were sampled for microplastic densities (Figure 1). The six sites were selected based on accessibility when using the manta trawl, and their location along the rivers (upstream and downstream of Winnipeg's three wastewater treatment plants: North End Water Pollution Control Centre (NEWPCC) and South End Water Pollution Control Centre (SEWPCC) on the Red River and the West End Water Pollution Control Centre (WEWPCC) on the Assiniboine River). The five inflow study sites were: Emerson (to assess contributions from the United States), Courchaine Road Bridge, Redboine Boat Club, the Forks Historic Rail Bridge (Forks), the Royal Manitoba Yacht Club (RMYC), and the outflow study site was the Nelson River in Norway House Cree Nation, Manitoba (Figure 1).

2.2 Surface Water Sample Collection, Processing, and Quantification

Surface water was sampled for microplastics using a manta trawl. The manta trawl has a net with a mesh size of 333 μm, is 295 cm long, has an aperture width of 61 cm, and a height of 18 cm. The trawl was deployed facing the rivers current off of bridges or docks. A total of 14 samples were collected from the six study sites in June (Redboine Boat Club, Forks and RMYC), July (Courchaine Road Bridge, Redboine Boat Club, Forks, and RMYC), October (Emerson, Redboine Boat Club, Forks, RMYC) (2016) and May (Nelson River) (2017). The variation in numbers of samples per site was due to logistical issues such as weather and time constraints. The four months were chosen opportunistically and sampled based on field season availability. Seasonality effects may play a role in the densities of microplastics across sites. Variation in

sampling sites was accounted for by grouping sites into categories (upstream versus downstream) and using a flow meter to correct for differences in water flow across sampling sites and times. The shorter sampling time in June was a result of high river flows, making longer deployments of the manta trawl very challenging. Materials captured by the trawl were passed through a 355 μm sieve using MilliQ water. Debris retained in the sieve was placed into labelled mason jars and preserved with 70% ethanol for future processing and analysis.

At time of analysis, samples were filtered through a 355 μm mesh brass sieve and rinsed with deionized (DI) water to remove the ethanol. DI water was added to the sample to reconstitute it to 1,250 mL and a subsample of 250 mL was collected and processed using a wet peroxide oxidation (WPO) treatment (Masura et al., 2015; Mason et al., 2016). The 250 mL subsample was stirred and heated to 75°C, followed by 20 mL additions of a 0.05 M Fe (II) solution and 30% hydrogen peroxide (H_2O_2) to facilitate chemical digestion of organic material. All digestions were conducted in a laminar flow hood. At approximately 10 minute intervals, samples were re-examined and additional H_2O_2 was added. The process was repeated until all organic material was digested. Samples were covered and left for 24 hours to digest fully. Blanks were deployed to account for possible airborne and waterborne (in our DI water) microplastic contamination from the lab while samples were digested and enumerated. The WPO treatment has the potential to digest some of the microplastics within our samples as temperatures are elevated to (>80°C) immediately after peroxide additions.

After filtering the sample through the sieve and rinsing with DI water to remove H_2O_2, the contents were placed into glass Petri dishes. The number and type of microplastic particles were visually examined in the Petri dish using a dissecting microscope. Microplastics were counted and types were recorded. Our microplastic particles were categorized into five shape categories: fragments (hard with jagged edges), foams (sponge-like and light weight), fibres (thin lines), pellets (hard and spherical in shape), and films (thin and flimsy) (Figure 2). These types were part of our primary search pattern based on their presence in other marine and freshwater samples reported in the literature (e.g., Eriksen et al. (2013), Anderson et al. (2017), Baldwin et al. (2016)). Microplastic particles were transferred using a fine-tipped probe to a glass vial containing ethanol and sealed with a rubber stopper for long-term storage. The number of microplastic particles collected was calculated for each trawl and used to calculate the densities of microplastics/km^2.

The same methods, lab, and personnel were used to visually sort and identify the microplastics as Anderson et al. (2017). That study found a 78% success rate at identifying plastic visually compared with the examination of samples using scanning electron microscopy and energy dispersive X-ray spectroscopy (Anderson et al., 2017). The densities of microplastics reported here were corrected for this identification bias (microplastic densities multiplied by 0.78).

2.3 Fish Collection, Processing, and Quantification

Fish were collected at Selkirk Park in Selkirk, Manitoba (Figure 1) following approved collection protocols (F16-029). Two fish species, *Cyprinus carpio* (common carp) and *Sander canadensis* (sauger) were obtained with the help of the Department of Fisheries and Oceans Canada's electrofishing boat in October 2016. The two fish species were selected as they occupy different ecological niches. Carp are a benthic filter feeder and sauger are a pelagic predatory species. Sampling took place near the shoreline and the fish were captured using long dip nets after being electroshocked and having floated to the surface of the water. The fish were then placed in a water bath and euthanized on site using an overdose of tricaine methylsulfate (TMS-MS-222). The fish were placed into freezer bags, placed on ice, and transported back to the University of Manitoba. The fish were placed in a freezer at -20°C for later processing. After thawing, nine sauger and eight carp were weighed and fork and total lengths were measured.

The fish were then dissected and the whole gastrointestinal tract removed from the esophagus to the anus. The entire gastrointestinal tract for each fish, fully intact, was processed using the same WPO method to digest organic material (Masura et al., 2015), with a small adjustment to deal with the high fat content of the fish. Right after the sample was processed for the first time, the sample was sieved and processed again. The samples were also rinsed with a solvent (ethanol)

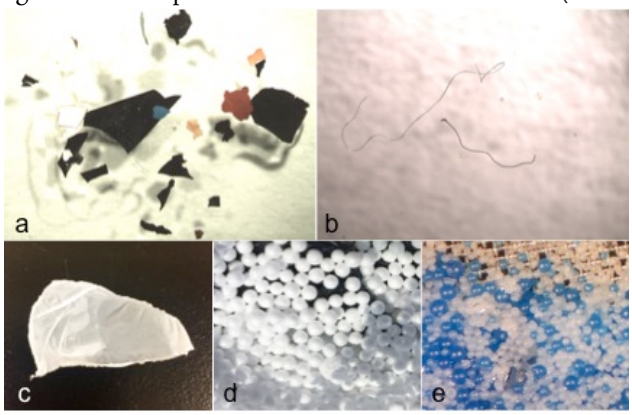

Figure 2: *The five shapes of microplastics: (a) fragments, (b) fibres, (c) films, (d) foams, (e) pellets. Photo credit: Sarah Warrack, University of Manitoba.*

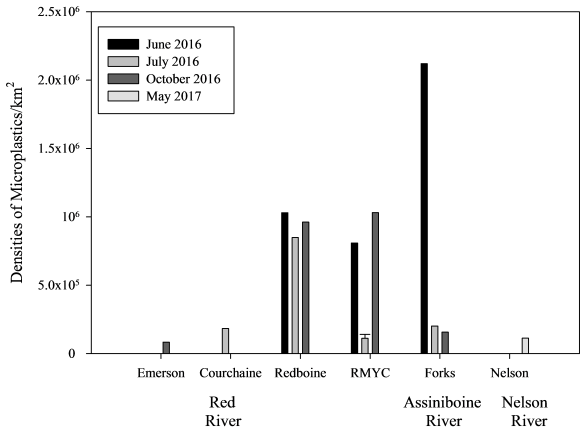

Figure 3: *Densities of microplastics/km^2 calculated for each sampling date at four Red River sites arranged South to North in direction of flow: Emerson, Courchaine Road Bridge, Redboine Boat Club, and the Royal Manitoba Yacht Club (RMYC), the Assiniboine River at the Forks, and the Nelson River. Density calculations were determined based on the number of microplastics counted in a given sample and the approximate surface area sampled by the manta trawl over a given deployment time. A triplicate sample was collected in July at the RMYC, the average and standard error calculated was 112,002 ± 29,339 microplastics/km^2.*

when sieving to get rid of any excess fat that the WPO did not digest. Once all organic material was digested, the contents were sieved, placed into glass Petri dish, and the number and type of microplastic particles were visually examined using a dissecting microscope. The number of microplastics found within each individual fish's digestive tract was counted and transferred to ethanol in a glass vial with a rubber stopper for long-term storage.

2.4 Blanks

Lab blanks were used to determine possible contamination from either air or DI water. DI water blanks were run under the DI water tap at a rate of eight L/min (480 L total) at the University of Manitoba for 60 minutes using a clean 355 μm brass sieve. Air blanks were employed by leaving one L mason jars of Milli-Q water out on the lab counter for 24 hours.

2.5 Data Analysis

Microplastic densities (microplastics/km^2) were analyzed by a Student's *t*-test using densities and site location (upstream versus downstream of wastewater treatment plants) as variables. A Pearson linear correlation was used to evaluate association between river velocity and the density of microplastics sampled, as well as association between sewage discharge and flux of microplastics in the river. The latter was analyzed using Z-scores, calculated for both flux and discharge (value – mean / standard deviation). Standardizing the data using the Z-score allowed for comparisons across sites. The flux calculation was used to understand the amount of microplastics in a cross-sectional area in the rivers at a given time, accounting for differences in discharge volume at different sampling sites. Discharge (m^3/sec) data was obtained from the Government of Canada's hydrometric monitoring data (Government of Canada: Water Office, 2017). A station (closest to our site) was selected and an average of the daily maximum and minimum discharge values were taken. Linear regression was used to compare counts of ingested microplastics with fish weight. A Student's *t*-test was also used to compare the number of microplastics ingested by the two fish species to help determine if fish species had different rates of microplastic ingestion. All statistical analyses were conducted using Sigma Plot with statistical significance considered for $p < 0.05$.

3 Results

3.1 Quality Assurance and Quality Control

The DI water blanks contained 13, 5, 16, and 9 particles (all fibres). These data suggest that on average, in our laboratory, one microplastic fibre is introduced for every 48 L of DI water used when processing the samples. The average rinse time of a sample is five minutes with DI water (at eight L/minute), with reconstitution to 1.25 L prior to subsampling, resulting in, on average, an estimated 0.85 fibres introduced to our samples from DI water alone. Two air blanks recorded eight and seven fibres over the 24 hour time period, or 0.3 fibres/hour. With an average microscope analysis time of four hours, we estimate that on average 1.25 microplastic particles were introduced from the lab air. In total, while processing samples, about two fibres/sample were likely introduced due to DI water and air. All water and fish sample counts were corrected by this blank contamination factor (two subtracted from all fibre counts). This contamination of microplastics likely affected the overall counts of microplastics in the gastrointestinal tract contents of fish more significantly than surface water samples, since the counts in fish were much lower than in samples (e.g., $\leq$ six fibres per fish).

Triplicate samples were taken at the Red River site, RMYC (downstream of NEWPCC) in July, where the manta trawl was deployed three times to evaluate within-site variability. The three densities of microplastics in the triplicates were: 161,275; 59,771; and 114,960 microplastics/km^2. The average and standard error calculated for RMYC in July was 112,002 ± 29,339 microplastics/km^2.

3.2 Surface Water

Microplastics were found in samples from all sites. Within the Red River inflow there was an average surface density of 632,489 microplastics/km^2 (n=8), and within the Assiniboine River inflow there was an average surface density of 812,672 microplastics/km^2 (n=3) across all sampling sites and dates (Figure 3). Density calculations were determined based on the number of microplastics counted in a given sample and the approximate surface area sampled by the manta trawl over a given deployment time. Surface area was calculated from the distance trawled, determined using a General Oceanics 2030R mechanical flow meter, and the width of the manta net opening (61 cm). A fundamental assumption to these calculations is the fact that while we report surface densities, in fact, there is a volume of water being sampled. One third of the net was deployed below the surface of the water during deployment, which was used to calculate the volume of water sampled. To remain consistent with the current literature, we report both microplastic surface (Eriksen et al., 2013; Anderson et al., 2017) and volume densities (Baldwin et al., 2016) (Table 1). The greatest inflow densities of microplastics/km^2 in the Red River were observed in June, downstream of the SEWPCC (1,030,091 microplastics/km^2) and October downstream of the NEWPCC (1,030,922 microplastics/km^2). In the Red River, the density of microplastics collected in June and October increased with the direction of flow from south

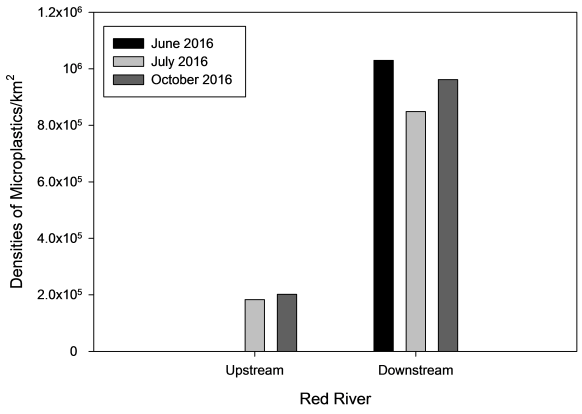

Figure 4: *Mean densities of microplastics/km^2 in the Red River upstream and downstream of the South End Water Pollution Control Centre (SEWPCC). No upstream site was sampled in June 2016 (preliminary sampling). Upstream SEWPCC sites: Emerson and Courchaine Road Bridge, and downstream SEWPCC site: Redboine Boat Club.*

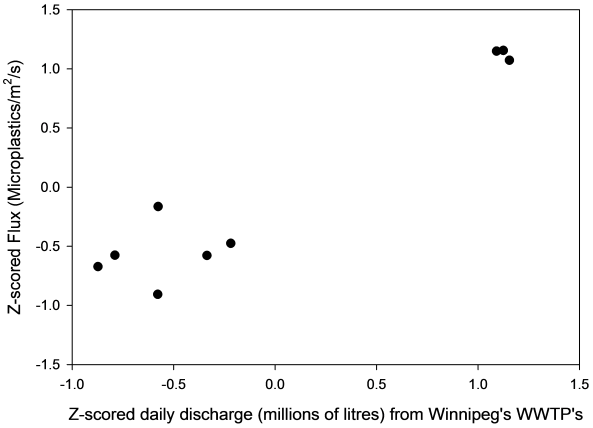

Figure 5: *Z-scored river flux of microplastics from the Red and Assiniboine rivers associated with Z-scored Waste Water Treatment Plant (WWTP) flux confirmed significant relationship (Pearson Linear Correlation: r=0.96, n=9, p-value=0.00005). Redboine was sampled downstream of the South End Water Pollution Control Centre, the Forks was sampled downstream of the West End Water Pollution Control Centre and Royal Manitoba Yacht Club (RMYC) was sampled downstream of North End Water Pollution Control Centre.*

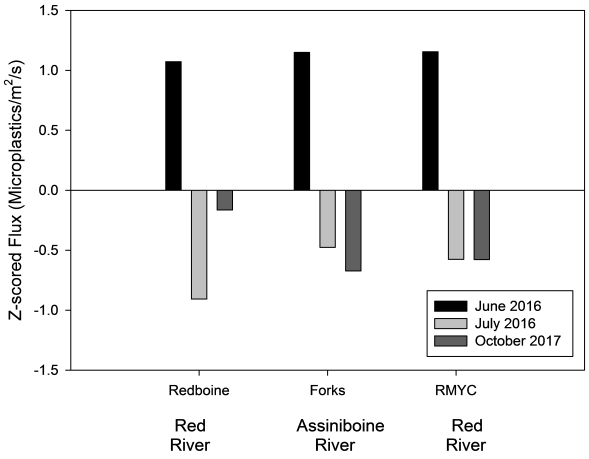

Figure 6: *Flux of microplastics/m^2/s (Z-scored) within the Red and Assiniboine rivers as a function of season (summer/ fall) where flux of microplastics/m^2/s was higher in early summer (June 27), and lower in both mid-summer and fall (July and October). Redboine was sampled downstream of the South End Water Pollution Control Centre (SEWPCC), the Forks was sampled downstream of the West End Water Pollution Control Centre (WEWPCC), and Royal Manitoba Yacht Club (RMYC) was sampled downstream of North End Water Pollution Control Centre (NEWPCC).*

Table 1: *Microplastic densities in surface areas (microplastics/km^2) and volume (microplastics/m^3) for Emerson, Courchaine, Redboine, Royal Manitoba Yacht Club (RMYC) and the Forks. The sites are arranged from south to north on the Red River.*

Date	Site	River	Surface Area Densities	Volume Densities
06-Oct-16	Emerson	Red	65,626.93	0.70
07-Jul-16	Courchaine	Red	143,201.90	1.53
27-Jun-16	Redboine	Red	806,763.83	8.62
07-Jul-16	Redboine	Red	667,045.81	7.13
06-Oct-16	Redboine	Red	751,743.85	8.03
27-Jun-16	RMYC	Red	631,540.63	6.75
07-Jul-16	RMYC	Red	126,142.26	0.94
06-Oct-16	RMYC	Red	808,549.79	8.64
27-Jun-16	Forks	Assiniboine	1,655,485.65	17.69
07-Jul-16	Forks	Assiniboine	157,686.44	1.69
06-Oct-16	Forks	Assiniboine	122,920.24	1.31
04-May-17	Nelson	Nelson	88,832.44	0.95

to north (Figure 3). In October, the density of microplastics along the southern part of the Red River was lower (Emerson site) and plateaued as sites moved north (Redboine Boat Club, RMYC). The densities of microplastics in the Assiniboine River sampled at the Forks in June 2016 had the greatest density of microplastics of all the sites (2,120,066 microplastics/km^2). In the Assiniboine River, the densities of microplastics decreased from June to October. The Nelson River had 88,832 microplastics/km^2, when sampled in May. The estimated daily inflow of microplastics from the Red River into Lake Winnipeg is 1,100,000 microplastics, so the Red River is contributing 401,500,000 microplastics annually to Lake Winnipeg, which contains a total of about 4,800,000,000 microplastics (Anderson et al., 2017). The estimated daily outflow of microplastics from Lake Winnipeg to the Nelson River is 10,800 microplastics, therefore the Nelson River is taking out 3,942,039 microplastics from Lake Winnipeg annually.

In the Red River, upstream of the SEWPCC (July 2016 and October 2016) the microplastic densities were significantly different from downstream of the SEWPCC, potentially due to wastewater inputs (Figure 4; one-tailed t-test, d.f= 3, p=0.00093). The Assiniboine River enters the Red River at the Forks, which is upstream of the RMYC.

A linear regression indicated no significant relationship between microplastic densities (microplastics/km^2) and river velocity (R^2=0.00003, n=14, p-value=0.98). In contrast, there was a significant correlation between the standardized (Z-scored) volume of wastewater treatment plant discharge and standardized (Z-scored) microplastic flux in the Red and Assiniboine rivers at regions near wastewater treatment plants (Pearson Linear Correlation: R=0.96, n=9, p-value=0.00005) (Figure 5). Flux of microplastics in the Red and Assiniboine followed a seasonal pattern of highest in spring (June) and lower in both summer and fall (July and October) (Figure 6), as was discharge from wastewater treatment plants.

The most common type of microplastics across all sites was identified as fibres (89%) (Figure 7). Pellets (0.2%), foams (0.32%), and films (0.2%) were the least common microplastic types detected (Figure 7).

3.3 Fish

Plastics were detected in seven of nine sauger; however, when corrected for possible contamination during processing, only four of nine sauger contained plastic. The average (corrected) count of microplastics within the nine sauger were one microplastic particle per fish. The average weight of sauger was 232.7 $\pm$ 17.2 grams and average fork length was 23.5 $\pm$ 2.9 cm (total length was 29.3 $\pm$ 0.9 cm). Linear regression indicated no significant relationship between the counts of microplastics and sauger size (R^2=0.06, n=9, p-value=0.53).

Plastics were detected in eight of eight carp, and when corrected for possible contamination during processing, only seven of eight carp contained plastic. The average (corrected) count of microplastics within the eight carp were seven microplastic particles. The average weight of the carp was 3849.5 $\pm$ 17.2 grams and average fork length was 55.2 $\pm$ 0.97 cm (total length was 60.5 $\pm$ 0.93 cm). Linear regression revealed that there was no significant relationship between counts of microplastics and carp size (R^2=0.04, n=8, p-value=0.64).

Significant differences in the number of ingested microplastics were observed for sauger (1 ± 1.5, n=9) and carp (7.1 ± 7, n=8) collected within the Red River, Manitoba, Canada in October 2016 (Student's t-test two-tailed α=0.05, d.f=15, p=0.01). Both carp and sauger had ingested fibres and fragments. Only one carp had ingested a film. Of the 17 fish processed, 65% contained plastic (44% of sauger and 88% of carp).

4 Discussion

4.1 Surface water

Microplastics were present in the surface waters of the 14 samples examined and contained on average 806,352 microplastics/km^2 (Red River), 1,241,085 microplastics/km^2 (Assiniboine River), and 113,888 microplastics/km^2 (Nelson River) (Table 1).

The densities of microplastics in these rivers (Table 1) are comparable to those in other rivers reported elsewhere. In the Rhine River in Germany, 892,277 microplastics/km^2 were reported (Mani et al., 2015). Four estuarine rivers in Chesapeake Bay, USA found average densities of microplastics to range between 40,852 and 155,374 microplastics/km^2 (Yonkos et al., 2014). Volumetric estimates of microplastics within the Red, Assiniboine and Nelson rivers ranged from 0.7 microplastics/m^3 to 18 microplastics/m^3, with an average of 5.3 microplastics/m^3 (Table 1). These estimates are also comparable to those reported for Great Lakes tributaries which ranged from 0.5 to 32 microplastics/m^3 with an average of 4.3 microplastics/m^3 (Baldwin et al., 2016). Some evidence exists to suggest that microplastic densities are higher in rivers with greater population density (Yonkos et al., 2014). We also found this to be the case in our study, where the density of microplastics was lower in the Nelson River (downstream of Norway House, population approximately 5,000), compared to the Red River (Winnipeg, population approximately 700,000). In addition, microplastics appear to be at lowest densities at higher latitudes (Lusher et al., 2015). Plastics have an anthropogenic origin, and as latitude increases, human population densities decrease (Browne et al., 2011; Eriksen et al., 2013).

Of note is that the inflow densities in the Red and Assiniboine rivers are four to six times greater than densities observed in Lake Winnipeg (200,000 microplastics/km^2) (Anderson et al., 2017), whereas the outflow densities are only 50% of the mean lake wide density. This large negative gradient in surface densities from the Red River, through Lake Winnipeg and into the Nelson is highly suggestive of significant losses due to settling within the lake. While inputs from the Saskatchewan River and Winnipeg River are not quantified here, they together contribute nearly 75% of the water input to Lake Winnipeg (Manitoba Water Stewardship, 2011). Thus, water inputs from these other tributaries may act to dilute inputs from the Red, or, if microplastic densities in these other tributaries are comparable, it suggests that Lake Winnipeg could be an even greater sink for microplastics in this system than suggested by the current study.

Densities of microplastics in the surface waters of the Red and Assiniboine rivers appear to be influenced by daily discharge of effluent from Winnipeg's three wastewater treatment plants (Figure 5). If so, our findings are consistent with other studies that have found significant correlation between wastewater treatment plant discharge and densities of microplastics (A. R. McCormick et al., 2016). Densities of microplastics were greater downstream of the SEWPCC (Figure 4) which is consistent with a study conducted in Illinois, United States which found greater microplastic densities downstream of wastewater treatment plants compared to upstream in seven of nine rivers ($p \leq 0.001$) (A. R. McCormick et al., 2016). Seasonality may be driving the correlation between wastewater treatment plant and density of microplastics in the surface waters of the rivers (Yonkos et al., 2014) as June had the highest wastewater treatment plant daily discharge of raw effluent for each of Winnipeg's three wastewater treatment plants' and June also had the highest flux of microplastics within the Red and Assiniboine rivers. Further investigation is required to better understand seasonal trends in microplastic densities in these rivers.

Microplastics in surface waters are influenced by wind (Browne et al., 2011) and rain events (Moore et al., 2011) as they can transfer terrestrial debris into the waterway, increasing the amount of microplastics in the system (Yonkos et al., 2014). Microplastic densities were elevated in June for the Red and Assiniboine rivers (Figure 3), which may be attributed to rain that occurred a few days before sampling. For the June 27, 2016 sampling, it rained June 24-26 and rainfall ranged from a low of 4.3 mm to a high of 39.4 mm (City of Winnipeg, 2017). July 7, 2016 rainfall ranged from a low of 0.3 mm to a high of 30.4 mm (City of Winnipeg, 2017). For the October 6, 2016 sampling it rained October 4th and 5th, ranging from a low of 7.8 mm to a high of 23.3 mm (City of Winnipeg, 2017). Therefore it rained more in June than July and October, which may have added to the higher densities of microplastics in June.

Fibres were the predominant type of microplastic particles found in the surface waters of the rivers sampled here (89%) (Figure 7). Other studies in freshwater (both rivers and lakes) have also found the majority of particles in their samples to be fibres (71% to 86%) (Baldwin et al., 2016; An-

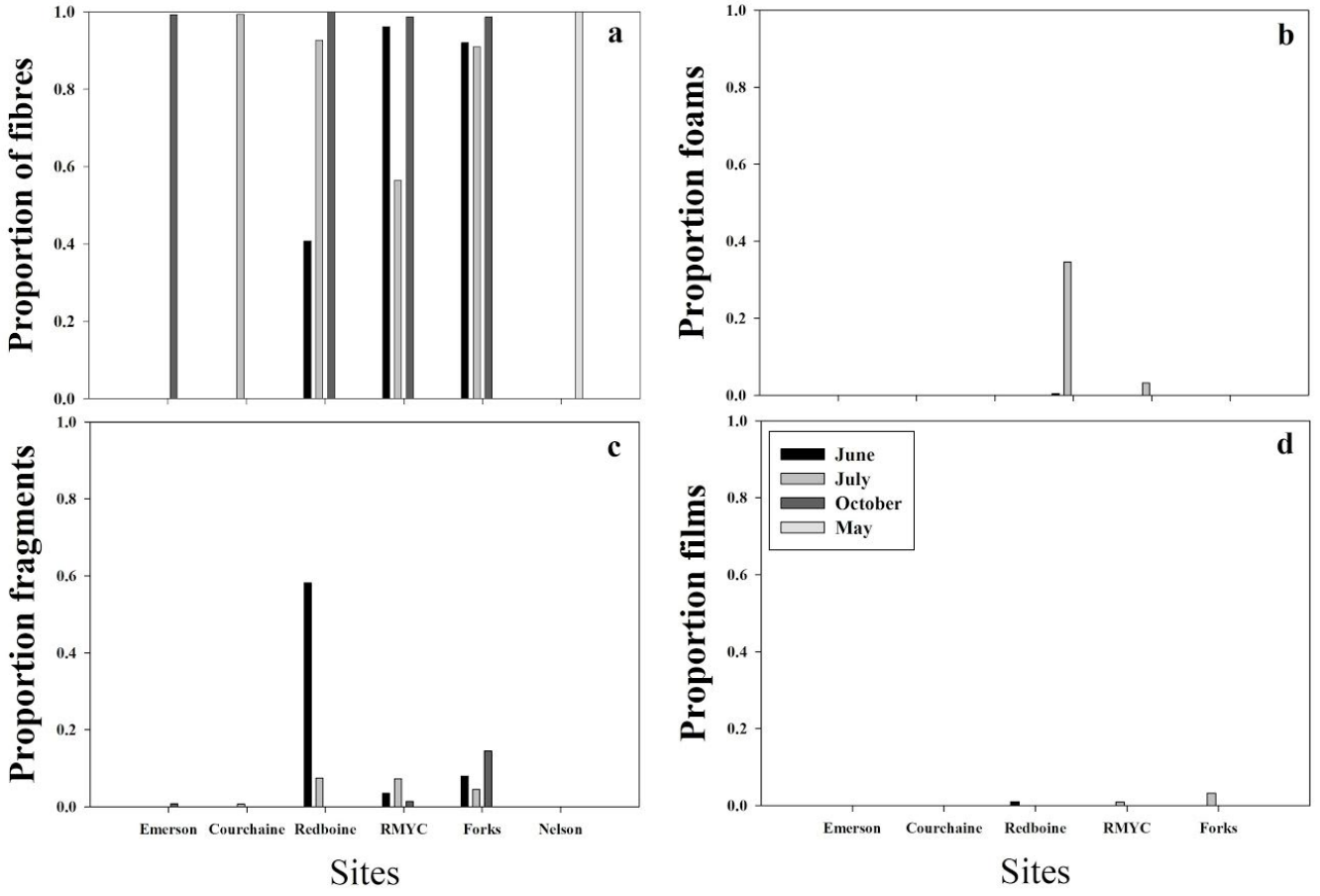

Figure 7: *The proportion of the four types of microplastic particles a) fibres, b) foams, c) fragments, and d) films, found at the 6 sites. Red River sites were Emerson, Courchaine, Redboine, and Royal Manitoba Yacht Club (RMYC), the Assiniboine River site was the Forks, and the Nelson River site. The Nelson River site only contained fibres.*

derson et al., 2017; Campbell et al., 2017). It remains unclear whether wastewater effluent is a primary source of microplastic fibres. Some studies have found that wastewater effluent is a significant source of fibres (Browne et al., 2011; A. McCormick et al., 2014; Mason et al., 2016), while other studies have found that wastewater treatment plants are effective at removing plastic particles (primarily fibres) as most if not all particles settle out in the sludge (Carr et al., 2016; Dris et al., 2016). However, the remaining 1.5% of plastic particles in wastewater treatment plant effluent still results in a major source of millions of microplastics discharged to rivers daily (Mason et al., 2016).

Our analysis suggests that large amounts of microplastics are being deposited in Lake Winnipeg sediments every year. The estimated total surface density of microplastics in Lake Winnipeg appears to be constant at approximately 4.8 billion from 2014 to 2016 (average density of microplastics over three years of study aproximately 200,000 microplastics/km^2 (Anderson et al., 2017) with a surface area of the lake approximately 24,000 km^2). Based on an estimate of daily flux from the RMYC (site closest to inflow of Lake Winnipeg) of 20,000 microplastics per day, and an estimated 55 m^2 cross sectional area of the Red River at RMYC, we estimate the annual input of microplastics from the Red and Assiniboine rivers is roughly 0.4 billion particles. By comparison, flux estimates from the Nelson River indicate that only 0.004 billion microplastics (1.0% of the input from the Red and Assiniboine rivers) are lost annually through the Nelson River (outflow of Lake Winnipeg). If we assumed that the contributions of other tributaries to Lake Winnipeg provided negligible amounts of microplastics (a highly conservative assumption), then the riverine input from the Red and Assiniboine rivers of 0.4 billion microplastics annually is three orders of magnitude greater than the measured loss

from the Nelson River, leaving 99% of the microplastics entering the lake through the Red River unaccounted for. The inclusion of any potential additional inputs (e.g., from the South Saskatchewan River) would only increase this loss rate even higher. One possible route for losses of microplastics is settling or sedimentation. Very little is currently known about sedimentation rates of microplastics, and our results strongly suggest value in pursuing investigations into quantifying microplastic settling rates and determining what mechanisms influence settling.

4.2 Fish

Microplastic ingestion by fish in the Red River was species-dependent. Carp had an average of seven microplastic particles whereas sauger had an average of one microplastic particle in their gastrointestinal tracts at the time of sampling. This difference between species may be due to their feeding strategy. Microplastic ingestion may be occurring accidentally when the fish are feeding (Lusher et al., 2013) or breathing. Carp are benthic feeders, and ingest all particles from the bottom layer of the river; non-food particles (sediments and plastics) are released through their gills (Food and Agriculture Organiation of the United Nations, 2017). As carp do this, they stir up the sediments, possibly re-suspending microplastics that have settled (Food and Agriculture Organiation of the United Nations, 2017). Sauger are predators, and may be less likely to encounter plastics compared to filter-feeding carp, and therefore ingest lower densities of microplastics.

Our findings differed from Lusher et al. (2013) who found no significant difference between the amount of microplastics in benthic versus pelagic fish in the English Channel (saltwater). Lusher et al. (2013) found that both pelagic and benthic fish species ingested 1-2 microplastics on average and total ingestion ranged from 1-15 microplastics. Our study found ingested microplastic particles ranging from 1-24. About 65% of all fish had ingested microplastics in our study (after blank corrections), compared to Lusher et al. (2013) where only 37% of all fish had ingested microplastics. This also suggests that there may be more microplastics in the sediments of the rivers, and future sampling should focus on sediment sampling of microplastics. No studies have been conducted on excretion of microplastic particles, so we are unsure of how many particles fish are ingesting throughout their life. The presence of plastics within the fish at the moment of sampling only indicates that the fish have recently ingested plastic (Foekema et al., 2013). The microplastic particles are as small as, or even smaller than, what fish typically eat. Therefore, it is not likely that fish are retaining these particles and they are most likely being excreted with the other waste products (Foekema et al., 2013). The particles are too small for the fish sampled in this study to likely feel satiated, cause intestinal blockage, or be in the fish long enough to be a vector of harmful contamination (Foekema et al., 2013). Due to the low numbers of microplastics fish in the Red River ingested, it does not appear likely that plastics affect body condition in this study.

In this study, the amount of microplastics ingested by two fish species (carp and sauger) differed (7.1 ± 7 and 1 ± 1.5) and feeding strategy may explain the difference. Campbell et al. (2017) did not find significant differences in the number of microplastics in the gastrointestinal tracts of different benthic and planktivorous fish species, yet northern pike, an apex predator, ingested the most microplastics. This higher density of microplastics may be due to trophic transfer of microplastics from ingested prey species (Campbell et al., 2017).

5 Conclusions

Microplastics were found in the Red, Assiniboine, and Nelson rivers. The majority of microplastics found in the rivers were fibres (89%). Other studies have also found that the majority of plastic particles are fibres (Baldwin et al., 2016; Anderson et al., 2017; Campbell et al., 2017). There were significant differences in the densities of microplastics found upstream versus downstream of wastewater treatment plants in the Red River, suggesting that wastewater treatment plants are a point source of microplastics in surface waters (Eerkes-Merando et al., 2015). The long-range transport of microplastics in rivers is a major contributor to the input and output of microplastics within their watersheds (Anderson et al., 2017). The Red and Assiniboine rivers are contributing 0.4 billion microplastics annually to Lake Winnipeg, and appear to be the major contributors of microplastics to Lake Winnipeg.

Future research efforts should focus on quantifying settling rates and sedimentation processes of microplastics in freshwater systems (both rivers and lakes). Quantifying settling rates of microplastics will help to understand how long microplastics persist in both lentic and lotic environments, and the processes that increase their settling rate.

References

Anderson, P., Warrack, S., Langen, V., Challis, J., Hanson, M., & Rennie, M. (2017). Microplastic pollution in Lake Winnipeg, Canada. *Environmental Pollution*, *225*, 223-231.

Arthur, C., Baker, J., & Bamford, H. (2010). Proceedings of the international research workshop on the occurrence, effects, and

fate of microplastic marine debris. *NOAA Technical Memorandum NOS-OR&R-30*.

Baldwin, A. K., Corsi, S. R., & Mason, S. A. (2016). Plastic debris in 29 Great Lakes tributaries: Relations to watershed attributes and hydrology. *Environmental Science & Technology*, *50*(19), 10377-10385.

Browne, M. A., Crump, P., Niven, S. J., Teuten, E., Tonkin, A., & Thompson, R. (2011). Accumulation of microplastic on shorelines worldwide: Sources and sinks. *Environmental Science & Technology*, *45*(21), 9175-9179.

Browne, M. A., Galloway, T., & Thompson, R. (2007). Microplastic – An emerging contaminant of potential concern? *Integrated Environmental Assessment and Management*, *3*(4), 559-561.

Campbell, S. H., Williamson, P. R., & Hall, B. D. (2017). Microplastics in the gastrointestinal tracts of fish and the water from an urban prairie creek. *FACETS*, *2*, 395-409.

Carr, S. A., Liu, J., & Tesoro, A. G. (2016). Transport and fate of microplastic particles in wastewater treatment plants. *Water Resources*, *91*, 174-182.

City of Winnipeg. (2017). Rainfall report [data file]. Retrieved from http://www.winnipeg.ca/waterandwaste /drainageflooding/rainfallreports/default.stm.

Cole, M., Wedd, H., Lindeque, P. K., Fileman, E. S., Halsband, C., & Galloway, T. S. (2014). Isolation of microplastics in biota-rich seawater samples and marine organisms. *Scientific Reports*, *4*(4528), 1-8.

Driedger, A. G. J., Durr, H. H., Mitchell, K., & van Cappellen, P. (2015). Plastic debris in the Laurentian Great Lakes: A review. *Journal of the Great Lakes Research*, *41*(1), 9-19.

Dris, R., Gasperi, J., Saad, M., Mirande, C., & Tassin, B. (2016). Synthetic fibres in atmospheric fallout: a source of microplastics in the environment? *Marine Pollution Bulletin*, *104*(1-2), 290-293.

Eerkes-Merando, D., Thompson, R. C., & Aldridge, D. C. (2015). Microplastics in freshwater systems: A review of the emerging threats, identification of knowledge gaps, and prioritization of research needs. *Water Research*, *75*, 63-82.

Eriksen, M., Lebreton, L. C. M., Carson, H. S., Thiel, M., Moore, C. J., Galgani, F., ... Reisser, J. (2014). Plastic pollution in the world's oceans: More than 5 trillion plastic pieces weighing over 250,000 tons a float at sea. *PLoS One*, *9*(12), 1-15.

Eriksen, M., Mason, S., Cox, C., Zellers, A., Edwards, W., Farley, H., & Amato, S. (2013). Microplastic pollution in the surface waters of the Laurentian Great Lakes. *Marine Pollution Bulletin*, *77*(1-2), 177-182.

Europe, P. (2015). Plastics the facts 2014/2015: an analysis of European plastics production, demand and waste data. Available from http://www.plasticseurope.org/document/plastics—the-facts-2015.aspx.

Fischer, E. K., Paglialonga, L., Czech, E., & Tamminga, M. (2016). Microplastic pollution in lakes and lake shoreline sediments - A case study on Lake Bolsena and Lake Chiusi (central Italy). *Environmental Pollution*, *213*, 648-657.

Foekema, E. M., De Gruijter, C., Mergia, M. T., van Franeker, J. A., Murk, A. J., & Koelmans, A. A. (2013). Plastic in North Sea fish. *Environmental Science & Technology*, *47*(15), 8818-8824.

Food and Agriculture Organiation of the United Nations. (2017). Common carp - Natural food and feeding habit [online]. Available from http://www.fao.org/fishery/affris/species-profiles/common-carp/natural-food-and-feeding-habits/en/.

GESAMP. (2015). Sources, fate and effects of microplastics in the marine environment: a global assessment. *Reports and Studies GESAMP*, *90*, 1-96.

Government of Canada: Water Office. (2017). Real time hydrometric data. Retrieved from https://wateroffice.ec.gc.ca/ mainmenu/real_time_data_index_e.html.

Klein, S., Worch, E., & Knepper, T. P. (2015). Occurrence and spatial distribution of microplastics in river shore sediments of the Rhine-Main area in Germany. *Environmental Science & Technology*, *49*(10), 6070-6076.

Lusher, A. L., McHugh, M., & Thompson, R. C. (2013). Occurrence of microplastics in the gastrointestinal tract of pelagic and demersal fish from the English Channel. *Marine pollution Bulletin*, *67*(1-2), 94-99.

Lusher, A. L., Tirelli, V., O'Connor, I., & Officer, R. (2015). Microplastics in Arctic polar waters: The first reported values of particles in surface and sub-surface samples. *Scientific Reports*, *5*(14947), 1-9.

Mani, T., Hauk, A., Walter, U., & Burkhardt, P. (2015). Microplastics profile along the Rhine River. *Scientific Reports*, *5*, 179-188.

Mason, S. A., Garneau, D., Sutton, R., Chu, Y., Ehmann, K., Barnes, J., ... Rogers, D. L. (2016). Microplastic pollution is widely detected in us municipal wastewater treatment plant effluent. *Environmental Pollution*, *218*, 1045-1054.

Masura, J., Baker, J., Foster, G., Arthur, C., & Herring, C. (2015). Laboratory methods for the snalysis of microplastics in the marine environment: Reccomendations for quantifying synthetic particles in water and sediments. *NOAA Technical Memorandum NOSOR&R-48*.

McCormick, A., Hoellein, T. J., Mason, S. A., Schluep, J., & Kelly, J. J. (2014). Microplastic is an abundant and distinct microbial habitat in an urban river. *Environmental Science & Technology*, *48*(20), 11863-11871.

McCormick, A. R., Hoelleing, T. J., London, M. G., Hittie, J., Scott, J. W., & Kelly, J. J. (2016). Microplastic in surface waters of urban rivers: Concentration, sources, and associated bacterial assemblages. *Ecosphere*, *7*(11), 1-22.

Moore, C. J., Lattin, G. L., & Zellers, A. F. (2011). Quantity and type of plastic debris flowing from two urban rivers to coastal waters and beaches of Southern California. *Journal of Coastal Zone Management*, *11*(1), 65-73.

Romeo, T., Pietro, B., Peda, C., Consoli, P., & Andalaro, F. (2015). First evidence of presence of plastic debris in stomach of large pelagic fish in the Mediterranean Sea. *Marine Pollution Bulletin*, *95*(1), 358-361.

Schindler, D. W. (2009). Lakes as sentinels and integrators for the effects of climate change on watersheds, airsheds and landscapes. *Limnology and Oceanography*, *54*, 2349-2358.

Yonkos, L. T., Friedel, E. A., Perez-Reyes, A. C., & Ghosal, S. (2014). Microplastics in four estuarine rivers in the Chesapeake Bay, U.S.A. *Environmental Science & Technology*, *48*(24), 14195-14202.

DOI: 10.5203/pmuser.201730580

Evaluation of Punching Shear Strength Models for Glass Fibre-Reinforced Polymer (GFRP)-Reinforced Concrete (RC) Flat Plates Subjected to Unbalanced Moment-Shear Transfer

Jordan K. Carrette[1], Ehab El-Salakawy[1]

[1]Department of Civil Engineering, University of Manitoba, Winnipeg, Canada, R3T 2N2

Corresponding Author: Jordan K. Carrette (jordan.carrette@mail.utoronto.ca)

Abstract

The provisions for the punching shear strength of glass fibre-reinforced polymer (GFRP)-reinforced concrete (RC) flat plates in the current North American and Japanese standards were investigated based on a database of experimental results of both interior and edge slab-column connections. In total, the results of 39 slab-column connections ranging extensively in their geometric and material properties were collected from the literature and analyzed to assess the accuracy and validity of the code provisions. In addition, the applicability of eight proposed analytical models from the literature was verified against the results of the dataset. It was demonstrated that the Canadian and Japanese standards provide the most consistent and accurate predictions; however, the American guidelines highly underestimate the capacities. In contrast, many of the proposed analytical models yielded inconsistent and unsafe estimates when applied to both concentrically and eccentrically loaded interior and edge connections. The assumption of a linear stress variation proposed by the eccentric shear stress model was validated for GFRP-RC edge specimens subjected to unbalanced moment-shear transfer.

Keywords: reinforced concrete, punching shear, glass fibre-reinforced polymer, slab-column connection, two-way flat plate

1 Introduction

Two-way flat plate systems are susceptible to a brittle failure mode termed 'punching shear'. In general, the application of highly localized forces to the slab results in flexural and shear stresses that initiate inclined crack propagation, which in combination with circumferential cracking around the connection periphery, can cause the column to essentially punch through the slab. This sudden drop in connection capacity can lead to a progressive collapse mechanism as adjacent columns are required to support the additional loading (Wight & MacGregor, 2011).

The punching shear behaviour of flat slabs is very complex and, despite continued investigation, the fundamental failure mechanism of slab-column connections cannot be fully described by existing theories. For this reason, many of the proposed models and current code provisions are empirically based, and in most cases are derived through regression analyses of published data (Gu et al., 2016). Moreover, the use of non-corrosive GFRP bars in lieu of conventional steel reinforcement has made predicting connection capacity significantly more difficult as their mechanical properties are very distinct from those of steel. Therefore, it is not valid to simply apply the same design formulae for both reinforcement types. Coupled with the complexities mentioned above, further uncertainty is introduced when the loading pattern shifts from concentric to eccentric in the presence of an unbalanced moment. The nature of this problem warrants further research, and so it is the aim of this report to assess the accuracy and validity of the major code provisions and proposed prediction models when applied to both concentrically and eccentrically loaded specimens. Through this comparative study, it will be shown that, despite extensive investigation, there exists no universal agreement on which factors dominate the behaviour of GFRP-RC connections subjected to unbalanced moment-shear transfer.

1.1 Review of Punching Shear Equations

The following section outlines the punching shear equations used in this assessment. Furthermore, the eccentric shear stress model for combined shear and moment transfer is presented.

1.1.1 National Standards

The Canadian standard CSA S806-12 (Canadian Standards Association, 2012) specifies that the factored shear stress resistance of concrete, v_c, due to punching shear shall be taken as the minimum of Equation 1, Equation 2, Equation 3. Where β_c is the ratio of the long side to short side of the column, λ is a parameter used to account for concrete density (equal to 1.00 for normal density), ϕ_c is the resistance factor for concrete (equal to 0.65), E_f is the modulus of elasticity of the longitudinal GFRP reinforcement (MPa), ρ_f is the flexural reinforcement ratio for GFRP, $f_c^{'}$ is the compressive strength of concrete (MPa), α_s is a parameter used to ac-

count for the location of the column within the slab (equal to 4 for interior columns, 3 for edge columns, and 2 for corner columns), d is the effective slab depth (mm), and b_o is the length of the critical shear perimeter measured a distance $d/2$ from the column face (mm).

These equations are based on the punching shear equations for steel-RC slabs as outlined in the Canadian standard CSA A23.3-04 (Canadian Standards Association, 2004). El-Gamal et al. (2005) found that the neutral axis (NA) depth of the cracked section decreases considerably after cracking due to the relatively low modulus of elasticity of GFRP bars, and consequently, the shear strength of GFRP-RC slab systems becomes highly influenced by the flexural reinforcement ratio. To account for this, the term $E_f\rho_f$, known as the axial (or elastic) stiffness, was introduced in the Canadian standard CSA S806-12 (Canadian Standards Association, 2012).

$$v_c = 0.028(1 + \frac{2}{\beta_c})\lambda\phi_c(E_f\rho_f f_c^{'})^{\frac{1}{3}} \tag{1}$$

$$v_c = 0.147(0.19 + \alpha_s\frac{d}{b_o})\lambda\phi_c(E_f\rho_f f_c^{'})^{\frac{1}{3}} \tag{2}$$

$$v_c = 0.056\lambda\phi_c(E_f\rho_f f_c^{'})^{\frac{1}{3}} \tag{3}$$

$$V_c = \frac{4}{5}\sqrt{f_c^{'}b_o c} \tag{4}$$

$$k = \sqrt{2\rho_f n_f + 9\rho_f n_f)^2} - \rho_f n_f \tag{5}$$

The American guideline ACI 440.1 R-15 (ACI Committee 440, 2015) proposed Equation **4** and Equation **5** to calculate the punching shear capacity of two-way slabs reinforced with GFRP bars. Where V_c is the ultimate punching shear capacity, c, equal to kd, is the NA depth of the cracked section (mm), k is the ratio of the NA depth to reinforcement depth, and n_f is the modular ratio (quotient of modulus of elasticity of GFRP bars, E_f, and modulus of elasticity of concrete, E_c). It should be noted that the punching shear capacity, V_c, can be transformed to the punching shear stress, v_c, by simply dividing by bd.

Equation **4** was derived from the one-way shear model developed by Tureyen & Frosch (2003) and assumes that the uncracked concrete section is the only parameter effectively resisting applied shear forces; contributions from aggregate interlock and dowel action are presumed to be negligible. Furthermore, Equation **4** implicitly considers the influence of axial stiffness on the punching shear strength by calculating the NA depth of the cracked transformed section.

The Japanese standard JSCE-97 (Japan Society of Civil Engineering, 1997) developed Equation **6**, with variables defined by Equation **7** to Equation **10**, to account for the effects of the slab size, reinforcement type and ratio, and column size on the punching shear capacity. In these equations, f_{pcd} is the design compressive strength of concrete (MPa), γ_b is a safety factor set equal to 1.3, E_s is the modulus of elasticity of steel (MPa), and u is the perimeter of the loaded area (mm). Coefficients β_d, β_p, and β_r take into consideration the effect of slab depth, reinforcement ratio and type, and loaded area (column size) on the punching shear strength, respectively. The design compressive strength of concrete is calculated using Equation **10** and cannot exceed the imposed limit of 1.2 MPa and therefore does not consider the effect of high-strength concrete (HSC) on punching shear capacity.

$$v_c = \beta_d\beta_p\beta_r \times \frac{f_{pcd}}{\gamma_b} \tag{6}$$

$$\beta_d = \sqrt[4]{\frac{1000}{d}} \leq 1.5 \tag{7}$$

$$\beta_p = \sqrt[3]{100\rho_f\frac{E_f}{E_s}} \leq 1.5 \tag{8}$$

$$\beta_r = 1 + \frac{1}{1 + 0.25\frac{u}{d}} \tag{9}$$

$$f_{pcd} = 0.2\sqrt{f_c^{'}} \leq 1.2 \tag{10}$$

1.1.2 Additional Improvements

The Institute of Structural Engineers (IStructE, 1999), a British organization, recommended substitution of the steel reinforcement ratio with an equivalent GFRP ratio (or equivalent area of steel), defined as the product of the flexural reinforcement ratio (or actual GFRP reinforcement area) and the modular ratio (Equation **11**).

This GFRP ratio (Equation **11**) was substituted into the original punching shear equation for steel-RC slabs (Equation **12**) outlined in the British standard BS 8110-97 (British Standards Institution, 1997), to yield the modified version applicable for GFRP-RC slabs (Equation **13**). In these equations, ρ_s is the steel reinforcement ratio, f_{ck} is the cube concrete compressive strength (equal to $f_c^{'}/0.80$), and $b_{1.5}$ is

the length of the critical shear perimeter measured a distance $1.5d$ from the column face.

El-Ghandour et al. (1999) modified the ACI 318-95 (ACI Committee 318, 1995) punching shear equation for steel-reinforced flat slabs by introducing the cubic root of the modular ratio, or $(E_f/E_s)^{1/3}$. Equation **14** shows the original code equation and Equation **15** shows the modified version, which now accounts for the influence of flexural reinforcement on the punching shear capacity. Based on their experimental work with GFRP flat slabs, El-Ghandour et al. (2000) proposed a modification to the equivalent GFRP ratio (Equation **11**), through the inclusion of a strain correction factor (Equation **16**), where 0.0045 is the imposed strain limit for the GFRP reinforcement, and ϵ_y is the yield strain for the steel reinforcement. Substitution of Equation **16** into Equation **12** yields the revised formula (Equation **17**).

$$\rho_s = \rho_f \frac{E_f}{E_s} \tag{11}$$

$$V_c = 0.79(100\rho_s)^{\frac{1}{3}}(\frac{400}{d})^{\frac{1}{4}}(\frac{f_{ck}}{25})^{\frac{1}{3}}b_{1.5}d \tag{12}$$

$$V_c = 0.79(100\rho_f \frac{E_f}{E_s})^{\frac{1}{3}}(\frac{400}{d})^{\frac{1}{4}}(\frac{f_{ck}}{25})^{\frac{1}{3}}b_{1.5}d \tag{13}$$

$$V_c = 0.33\sqrt{f_c'}b_o d \tag{14}$$

$$V_c = 0.33\sqrt{f_c'}(\frac{E_f}{E_s})^{\frac{1}{3}}b_o d \tag{15}$$

$$\rho_s = \rho_f \frac{E_f}{E_s}\frac{0.0045}{\epsilon_y} \tag{16}$$

$$V_c = 0.79(100\rho_f \frac{E_f}{E_s}\frac{0.0045}{\epsilon_y})^{\frac{1}{3}}(\frac{400}{d})^{\frac{1}{4}}(\frac{f_{ck}}{25})^{\frac{1}{3}}b_{1.5}d \tag{17}$$

Further modification of the British standard BS 8110-97 (British Standards Institution, 1997) was made by Matthys & Taerwe (2009) who proposed Equation **18**. This revision improves the prediction accuracy as it accounts for the relatively low modulus of elasticity of GFRP reinforcement by incorporating the equivalent reinforcement ratio (Equation **11**).

Ospina et al. (2003) proposed an empirical equation based on Equation **18**, which takes the square root of the modular ratio as opposed to the cubic root and omits the size effect factor, $(1/d)^{1/4}$. Based on the available test data, Ospina et al. (2003) found it unnecessary to correct the predicted punching shear capacity, by reducing it, to account for the size effect. Additionally, they observed that the square root of the modular ratio produced more accurate results than the cubic root, therefore justifying Equation **19**.

Zaghloul & Razaqpur (2004) recommended Equation **20** based on the one-way shear equation outlined in the previous version of the Canadian standard CSA S806-02 (Canadian Standards Association, 2002).

El-Gamal et al. (2005) observed that the punching shear strength is increased when the boundary conditions restrain the slab edges against movement. They found that the amount of slab restraining is dependent on the axial stiffness of the reinforcement, the in-plane stiffness of adjacent slabs, and the presence of a supporting beam at the slab edge. Based on their conclusions, El-Gamal et al. (2005) made modifications (Equation **21**–Equation **22**) to the ACI 318-05 (ACI Committee 318, 2005) code equation. Here, α is a factor to account for the axial stiffness of the reinforcement and is a function of the effective slab depth to critical shear perimeter ratio (d/b_o). Additionally, the effect of the boundary conditions on punching shear capacity is considered by multiplying Equation **14** by 1.2^N, where N is the slab continuity factor (equal to 0 for one span in both directions, 1 for slabs continuous along one direction, and 2 for slabs continuous along both directions).

$$V_c = 1.36\frac{(100\rho_f \frac{E_f}{E_s} f_c')^{\frac{1}{3}}}{d^{\frac{1}{4}}}b_{1.5}d \tag{18}$$

$$V_c = 2.77(\rho_f f_c')^{\frac{1}{3}}\sqrt{\frac{E_f}{E_s}}b_{1.5}d \tag{19}$$

$$v_c = 0.07\lambda\phi_c(f_c'\rho_f E_f)^{0.333}b_o d \tag{20}$$

$$V_c = 0.33\sqrt{f_c'}b_o d\alpha(1.2)^N \tag{21}$$

$$\alpha = 0.62(\rho_f \frac{E_f}{1000})^{\frac{1}{3}}(1 + \frac{8d}{b_o}) \tag{22}$$

The development of a purely analytical model to predict the ultimate punching shear strength of two-way slabs is hindered by the inherent complexities of the punching

shear problem. As mentioned previously, due to the three-dimensional nature of the problem, unknown shear transfer mechanisms and unknown contributions from the uncracked concrete, aggregate interlock, and dowel action at failure render the laws of statics and mechanics ineffective. Theodorakopoulos & Swamy (2008a) developed a unified design model which encompasses their former theories for steel-RC (Theodorakopoulos & Swamy, 2002) and GFRP-RC (Theodorakopoulos & Swamy, 2007) slab-column connections. This model is unique in that it was developed without the need for empirically-derived coefficients and considers the ultimate punching shear capacity of the slab to be governed by the moment-shear interaction of the flexural and shear critical sections.

Theodorakopoulos & Swamy (2007) extended their existing steel-RC model (Theodorakopoulos & Swamy, 2002) to be applicable for GFRP-RC slabs by accounting for differences in material properties and the bond-slip behaviour between the GFRP reinforcement and concrete matrix (Equation 23–Equation 24). In these equations, V_{uf} is the ultimate theoretical punching shear strength of GFRP slabs, f_{ct} is the tensile splitting strength of concrete (equal to $0.27f_{cu}^{2/3}$), θ is the angle of failure of the fracture cone surface (assumed to be 30°), ξ_s is a size effect factor (as expressed in Equation 24), b_p is the length of the critical shear perimeter measured a distance $1.5d$ from the column face, and $(X)_f$ is the combined NA depth for GFRP slabs. The authors argued that a larger critical shear perimeter would adequately account for the shear resistance provided by the aggregate interlock and dowel action.

Theodorakopoulos & Swamy (2002) further proposed that two NA depths exist within the slab section; namely, the depth of the compression zone of the flexural section, $(X_f)_f$, and the depth of the compression zone of the shear section, X_s. The former corresponds to the location of the inclined shear cracks, whereas the latter corresponds to the location of the flexural cracks. It is hypothesized that the ultimate punching shear capacity is governed by the interaction between the moment and shear of these two critical sections. The combined NA depth (Equation 25) is represented by the harmonic mean of the flexural and shear critical section depths.

Based on experimental data for steel-RC slabs (Theodorakopoulos & Swamy, 2002), it was proposed that the depth of the compression zone of the shear critical section be taken as Equation 26.

$$V_{uf} = f_{ct}cot(\theta)\xi_s b_p (X)_f \tag{23}$$

$$\xi_s = (\frac{100}{d})^{\frac{1}{6}} \tag{24}$$

$$(X)_f = \frac{2X_s(X_f)_f}{X_s + (X_f)_f} \tag{25}$$

$$X_s = 0.25d \tag{26}$$

$$\frac{(X_f)_f^*}{d} = \frac{\epsilon_{cu}}{\epsilon_{cu} + \epsilon_f^*} \tag{27}$$

$$\frac{(X_f)_f^*}{d} = \frac{\rho_f f_f}{k_1 f_{cu}} \tag{28}$$

$$\frac{\epsilon_f}{\epsilon_{fu}} = 0.55\times [\frac{-\epsilon_{cu}/\epsilon_{fu} + \sqrt{(\epsilon_{cu}/\epsilon_{fu})^2 + 4(1+\epsilon_{cu}/\epsilon_{fu})/(\rho_f/\rho_{fb})}}{2}] \tag{29}$$

Assuming a perfect bond between the GFRP reinforcement and the hardened concrete matrix, the condition of strain compatibility and force equilibrium yields the relationships shown by Equation 27 and Equation 28, respectively (Theodorakopoulos & Swamy, 2007).

To account for the case where bond-slip occurs between the GFRP reinforcement and hardened concrete matrix, the actual GFRP strain, ϵ_f, is taken to be a fraction of the GFRP strain calculated under the assumption of a perfect bond, ϵ_f^*. Based on the available literature addressing the bond characteristics of GFRP, Theodorakopoulos & Swamy (2007) ultimately proposed a 45% reduction in the actual GFRP strain, yielding Equation 29.

Finally, the depth of the NA of the flexural section can be determined using Equation 30 in conjunction with the value found from Equation 29. Theodorakopoulos & Swamy (2008b) further simplified their GFRP model by introducing two new parameters, α_f and λ_f. The refined model for GFRP-RC slabs is expressed by Equation 31, where V_{ufd} is the ultimate design punching strength of GFRP slabs, and α_f and λ_f are design parameters expressed by Equation 32 and Equation 33, respectively. The former parameter, α_f, considers the axial stiffness of the reinforcement, $\rho_f E_f$, the ultimate design tensile strain of GFRP, $\epsilon_{fud} = 3\epsilon_{cu} = 0.0105$, and the concrete cube strength, f_{cu}. It can be proven that α_f is essentially the ratio of the flexural reinforcement ratio, ρ_f, to the balanced flexural reinforcement ratio, ρ_{fb}. The latter

parameter, λ_f, considers the bond-slip strain reduction coefficient, k_f, and is itself a function of α_f. Together, these two parameters form the simplified expression for the combined NA depth shown in Equation **34**.

For the sake of generality, Theodorakopoulos & Swamy (2008b) subsequently modified their existing steel-RC model (Theodorakopoulos & Swamy, 2002) to include the design parameters α_s and λ_s, shown by Equation **36** and Equation **37**–Equation **38**, respectively. The ultimate design punching strength of steel-RC slabs, V_{usd}, is found by evaluating Equation **35**. It can easily be seen by comparison of Equation **31** (GFRP-RC design model) with Equation **35** (steel-RC design model), that both proposed equations retain the same structure, and together result in what Theodorakopoulos & Swamy (2008b) term their 'unified design method'.

Both models use an identical expression for the combined NA, as shown by Equation **34**, from which it is concluded that the ultimate punching shear capacity is dependent on the moment-shear interaction of the two critical sections. Furthermore, Equation **34** suggests that the flexural reinforcement ratio and the concrete strength do not exist as separate entities, but rather are co-dependent. This is contrary to many of the proposed prediction models outlined previously.

$$\begin{aligned}\frac{(X_f)_f}{d} &= \frac{\rho_f E_f}{k_1 f_{cu}}\epsilon_f \\ &= \frac{\rho_f E_{fu}}{k_1 f_{cu}}\frac{\epsilon_f}{\epsilon_{fu}} \\ &\text{for } \frac{\rho_f}{\rho_{fb}} \geq 0.33\end{aligned} \tag{30}$$

$$\begin{aligned}V_{ufd} &= \frac{1}{2}0.234 f_{cu}^{\frac{2}{3}}\xi_s \frac{2\alpha_f\lambda_f}{1+\alpha_f\lambda_f}b_p d \\ &\text{for } \alpha_f > 0.33\end{aligned} \tag{31}$$

$$\begin{aligned}\alpha_f &= \frac{\rho_f f_{fud}}{0.145 f_{cu}} \\ &= \frac{\rho_f E_f \epsilon_{fud}}{0.145 f_{cu}}\end{aligned} \tag{32}$$

$$\begin{aligned}\lambda_f &= \frac{\epsilon_f}{\epsilon_{fud}} \\ &= \frac{k_f}{6}(-1+\sqrt{1+\frac{48}{\alpha_f}}) < 1 \\ &\text{for } \alpha_f > 0.33\end{aligned} \tag{33}$$

$$(X)_f = \frac{2\alpha_f\lambda_f}{1+\alpha_f\lambda_f}(0.25d) \tag{34}$$

$$V_{usd} = \frac{1}{2}0.234 f_{cu}^{\frac{2}{3}}\xi_s \frac{2\alpha_s\lambda_s}{1+\alpha_s\lambda_s}b_p d \tag{35}$$

$$\alpha_s = \frac{\rho_s f_y}{0.145 f_{cu}} \tag{36}$$

$$\lambda_s = \frac{f_s}{f_y} \tag{37}$$

$$\lambda_s = \begin{Bmatrix} 1.60 - 0.75\alpha_s & 0.20 \leq \alpha_s \leq 0.50 \\ 1.35 - 0.25\alpha_s & 0.50 \leq \alpha_s \leq 1.00 \\ 1.20 - 0.10\alpha_s & 1.00 \leq \alpha_s \leq 2.50 \\ 1.30 - 0.14\alpha_s & 2.50 \leq \alpha_s \leq 5.00 \end{Bmatrix} \tag{38}$$

$$v_{max} = \frac{V_g}{A_c} + \frac{\gamma_v M_{unb}}{J_c}e \tag{39}$$

$$\gamma_v = 1 - \gamma_f \tag{40}$$

$$\gamma_f = \frac{1}{1+(\frac{2}{3})\sqrt{b_1/b_2}} \tag{41}$$

$$V_{max} = V_g + \frac{\gamma_v A_c e}{J_c}M_{unb} \tag{42}$$

1.2 Eccentric Shear Stress Model for Combined Shear and Moment Transfer

The behaviour and, consequently, the analysis of eccentrically loaded slab-column connections becomes significantly more complex with the introduction of unbalanced moments. Such loading cases arise when the slab-column connection is subjected to asymmetrical loading (gravity or lateral) and/or unequal slab spans, and result in a combination of flexure, shear, and torsion transferred from the slab to the column.

The traditional ACI design method, commonly referred to as the J_c Method, is based on a linear variation of shear stress and is implemented in both CSA S806-12 (Canadian Standards Association, 2012) and ACI 318-11 (ACI Committee 318, 2011). The maximum shear stress, v_{max}, acting on the critical section is given by Equation **39**, where V_g is the

factored direct shear force due to vertical loads, A_c is the critical shear section area (product of b_o, the length of the critical shear perimeter measured a distance $d/2$ from the column face, and d, the effective slab depth), γ_v is the fraction of the factored unbalanced moment, M_{unb}, that is being transferred to the critical shear section through shear stresses, J_c is a geometric property of the critical shear section analogous to the polar moment of inertia, and e is the distance between the centroid of the critical shear section and the location of the maximum shear stress.

Intuitively, in the absence of supporting beams or spandrels, all the applied loads acting on the slab must be transferred directly to the column, and thus the sum of the moment transferred by shear and that transferred by flexure must equal the total unbalanced moment being applied to the connection. This is expressed by Equation **40**, where γ_f is the fraction of the factored unbalanced moment, M_{unb}, transferred to the critical shear section by direct flexure, and is solely a function of the geometric properties of the column as shown in Equation **41**.

It can easily be shown that for an interior column with square geometry ($b_1 = b_2$), Equation **41** reduces to $\gamma_f = 0.60$; that is, 60% of the unbalanced moment is assumed to be transferred by flexure and the remaining 40% to be transferred by shear (Wight & MacGregor, 2011).

The eccentric shear stress model assumes that the shear stresses acting on the critical shear perimeter vary linearly with the distance from the centroidal axis of the critical perimeter. The total combined shear stress is taken to be the superposition of the direct shear stresses and the fraction of the unbalanced moment transferred by shear. To gain insight into Equation **39**, both sides can be multiplied by the critical shear section area, $A_c = b_o d$, to yield Equation **42**. When expressed in this form, it can be easily recognized that the eccentric shear stress model is nothing more than a linear equation having a y-intercept equal to V_g and slope equal to $\gamma_v A_c e/J_c$. Note that the slope in Equation **42** is an invariable number that is a function of the geometric properties of the slab-column connection, and, as a result, the maximum shear stress increases proportionally with the magnitude of the applied unbalanced moment (Song et al., 2012).

2 Methods

Data from 39 interior and edge slab-column connections were collected from published literature (El-Gendy & El-Salakawy, 2015; El-Ghandour et al., 1999, 2003; Gouda & El-Salakawy, 2015; Ospina et al., 2003; Hussein et al., 2004; Zaghloul & Razaqpur, 2004; Lee et al., 2009; Dulude et al., 2010; Nguyen-Minh & Rovňák, 2013). All the chosen specimens met the following selection criteria: (1) GFRP-reinforced two-way flat plates, (2) compressive concrete strength < 60 MPa, (3) square column geometry, (4) monotonic loading, (5) no transverse shear reinforcement, and (6) singly-reinforced with reinforcement in tensile zone only.

The three major code equations and eight proposed prediction models were applied to both concentrically and eccentrically loaded interior and edge connections. All reduction factors and safety factors were set equal to 1.00 during the analysis to predict the nominal punching shear strength. Also, the test-to-predicted shear strength ratio is presented for every equation. Three conclusions can be made based on the value of this ratio: (1) if $V_{TEST}/V_{PRED} = 1$, the model or code perfectly predicts the ultimate punching shear capacity; (2) if $V_{TEST}/V_{PRED} < 1$, the model or code overestimates the ultimate punching shear capacity; (3) if $V_{TEST}/V_{PRED} > 1$, the model or code underestimates the ultimate punching shear capacity. Therefore, based on the three cases mentioned above, the most desirable case is when the test-to-predicted ratio approaches unity.

3 Results & Discussion

3.1 Interior Specimens Concentrically Loaded

The test-to-predicted shear ratios are summarized in Table 1 for 29 interior connections. Note that two design provisions, ACI 318-05 (ACI Committee 318, 2005) and BS 8110-97 (British Standards Institution, 1997), are valid for steel-RC slab-column connections only and so serve as a reference.

The ACI guideline Equation **4** produced highly conservative results, with a mean of 2.003 and standard deviation of 0.276 (coefficient of variation (COV) = 13.76%). The design provision was developed based on the one-way shear equation proposed by Tureyen & Frosch (2003) and assumes that only the uncracked concrete contributes to the resistance of shear stresses. It completely neglects the contribution from the aggregate interlock and the dowel action of the reinforcing bars and therefore significantly underestimates the strength of the connection. The Canadian standard (Equation **1**–Equation **3**) and Japanese standard (Equation **6**) produce more accurate results of 1.046 ± 0.142 (COV = 13.60%) and 1.127 ± 0.163 (COV = 14.47%), respectively. Based on this sample group, the Canadian standard CSA S806 (Canadian Standards Association, 2012) is more accurate than the Japanese standard (Japan Society of Civil Engineering, 1997) at predicting the punching shear strengths of concentrically loaded interior slab-column connections reinforced with

Table 1: *Comparison between experimental and predicted strength for concentrically loaded interior slab-column connections from published literature.*

Code Provision (Equation #)	V_{TEST}/V_{PRED}		
	Mean	Std. Dev.	COV (%)
ACI 318[a] (14)	0.834	0.225	27.01
BS 8110[a] (12)	0.775	0.138	17.80
ACI 440 (4)	2.003	0.276	13.76
CSA S806 (Min 1-3)	1.046	0.142	13.60
JSCE 97 (6)	1.127	0.163	14.47
El-Ghandour et al. (15)	1.280	0.292	22.84
Matthys and Taerwe (18)	1.143	0.164	14.37
Ospina et al. (19)	0.978	0.153	15.64
El-Gamal et al. (21)	0.999	0.153	15.31
Theodorakopoulos and Swamy (23)	1.000	0.122	12.25
Zaghloul and Razaqpur (20)	0.905	0.123	13.61
IStructE (13)	1.194	0.172	14.37
El-Ghandour et al. (17)	0.955	0.137	14.37

[a] Code provision for steel-RC slab-column connections only.

GFRP. All three code provisions tend to underestimate, to varying degrees, the punching shear capacity. All the average test-to-predicted punching shear strengths lie above 1.00, indicating that the predicted capacity is less than the observed capacity, and thus are suitable for design purposes.

Both the Canadian standard and Japanese standard take the cubic root of the axial stiffness, $(\rho_f E_f)^{1/3}$, in their prediction equations. Additionally, the Canadian standard takes the cubic root of the compressive strength of concrete, whereas the Japanese standard takes the square root and imposes a limit on its design compressive strength. The governing CSA equation was always Equation **3**. For Equation **1** and Equation **2** to govern, the column aspect ratio, β_c, must be larger than 2 or the critical perimeter to effective slab depth, b_o/d, must be less than 20, respectively. However, the Japanese standard considers the effect of the slab size, reinforcement type and ratio, and column size by introducing three parameters, β_d, β_p, and β_r, respectively. Thus, the effect of these parameters is included in every prediction made by the Japanese design equation, whereas they are only included in the Canadian standard if they satisfy the specific constraints.

Equation **13** (IStructE, 1999), Equation **15** (El-Ghandour et al., 2000), and Equation **18** (Matthys & Taerwe, 2009) all produce underestimated capacities, whereas Equation **17** (El-Ghandour et al., 2000) and Equation **20** (Zaghloul & Razaqpur, 2004) yield overestimated predictions. Equation **19** (Ospina et al., 2003), Equation **21** (El-Gamal et al., 2005), and Equation **23** (Theodorakopoulos & Swamy, 2002) produce accurate predictions with average V_{TEST}/V_{PRED} ratios approximately equal to 1.00. Equation **15** (El-Ghandour et al., 2000) introduced the term $(E_f/E_s)^{1/3}$ into Equation **14** (ACI Committee 318, 1995) to develop their first model. Comparison of the results from Equation **14** and Equation **15** shows minor improvements. The unmodified Equation **14** does not produce conservative design results (predicted strength > test strength) with a mean of 0.834, whereas the modified ACI 318-05 (Equation **15**) (El-Ghandour et al., 2000) yields conservative results with a mean of 1.280. The introduction of the above term in Equation **14** results in a slightly larger standard deviation, but a lower COV.

ACI 318-05 (Equation **14**) (ACI Committee 318, 1995) was further refined by El-Gamal et al. (2005) (Equation **21**) by considering the axial stiffness of the bottom tensile reinforcement and the continuity of the slab. The authors showed that the punching shear strength is influenced by lateral constraints and boundary conditions. It was observed that the punching shear capacity of a slab is enhanced when it is restrained by adjacent slabs, as the slab edges are restricted from movement. The results of this analysis proved to support the modifications made by El-Gamal et al. (2005), yielding 0.999 ± 0.153 (COV = 15.31%). This is a significant improvement from the results produced by Equation **14** and Equation **15**.

Table 2: *Comparison between experimental and predicted strength for eccentrically loaded interior slab-column connections from Gouda & El-Salakawy (2015).*

Code Provision (Equation #)	V_{TEST}/V_{PRED}		
	Mean	Std. Dev.	COV (%)
ACI 318[a] (14)	0.820	0.136	16.56
BS8110[a] (12)	0.765	0.039	5.11
ACI 440 (4)	1.890	0.115	6.07
CSA S806 (Min. 1-3)	1.005	0.051	5.11
JSCE 97 (6)	1.126	0.074	6.59
El-Ghandour et al. (15)	1.174	0.194	16.56
Matthys and Taerwe (18)	1.049	0.054	5.11
Ospina et al. (19)	0.804	0.041	5.11
El-Gamal et al. (21)	0.926	0.083	8.94
Theodorakopoulos and Swamy (23)	0.917	0.053	5.76
Zaghloul and Razaqpur (20)	0.869	0.044	5.10
IStructE (13)	1.096	0.056	5.11
El-Ghandour et al. (17)	0.876	0.045	5.11

[a] Code provisions for steel-RC slabs only.

The current American guideline (Equation 4) for the ultimate punching shear of concrete slabs reinforced with GFRP bars or grids possesses the same form as that of ACI 318-05 (Equation 14). ACI 440 (Equation 4) considers the effect of reinforcement stiffness (axial stiffness) by means of calculating a cracked transformed section NA depth. This NA depth is a function of the flexural reinforcement ratio of the GFRP reinforcement as well as the modular ratio, the ratio of elastic modulus of GFRP to elastic modulus of concrete. Equation 21, proposed by El-Gamal et al. (2005), better represents the punching shear of concentrically loaded interior connections, in comparison to the current standard used in practice by ACI 440 (ACI Committee 440, 2015). All equations discussed above take the critical shear perimeter to be located at a distance of $d/2$ from the column face.

The British standard (Equation 12) applied directly to GFRP specimens underestimates the punching shear capacity, as expected based on the results of directly applying the ACI 318-05 code. Therefore, both steel codes yield higher predicted strengths compared to the actual or test strengths.

The British standard was first modified by Matthys & Taerwe (Equation 18) to account for the axial stiffness of the GFRP reinforcing bars. A substitution was made in the British standard for an equivalent steel ratio, $\rho_s = \rho_f E_f / E_s$. The effect of this substitution results in more accurate predictions of the punching shear (1.143 ± 0.164, COV = 14.37%). Ospina et al. (Equation 19) then modified the equation of Matthys & Taerwe (Equation 18) by taking the square root of the modular ratio E_f/E_s, instead of the cubic root. This improved the test-to-predicted ratio and slightly reduced the standard deviation, however an increase in the COV was observed. The Institute of Structural Engineers, UK (Equation 13) also proposed making the substitution in the British standard with an equivalent area of steel. El-Ghandour et al. (2000) proposed a second model (Equation 17) that introduced a different equivalent steel reinforcement ratio which imposes a strain limit of 0.0045 for GFRP. This substitution into the British standard yielded a mean of 0.955 ± 0.137 (COV = 14.37%). Comparison between the results from the Institute of Structural Engineers, UK (Equation 13) and El-Ghandour et al. (Equation 17), shows that the equivalent steel ratio proposed by El-Ghandour et al. (2000) produces results closer to the desired value of 1.00 and reduces the standard deviation slightly, with the COV remaining constant. For this set of equations discussed, the location of the critical shear perimeter is based on the British standard, and so measured a distance $1.5d$ from the column perimeter.

Zaghloul & Razaqpur (Equation 20) based their proposed equation on the one-way shear equation in the Canadian standard CSA S806-02 (Canadian Standards Association, 2012) and takes into consideration the axial stiffness of the reinforcing bars. This produced overestimated results with a mean of 0.905 ± 0.123 (COV = 13.61%). Of the 13

Table 3: *Comparison between experimental and predicted strength for eccentrically loaded edge slab-column connections from El-Gendy & El-Salakawy (2015).*

Code Provision (Equation #)	V_{TEST}/V_{PRED}		
	Mean	Std. Dev.	COV (%)
ACI 318[a] (14)	0.947	0.156	16.45
BS8110[a] (12)	0.877	0.076	8.62
ACI 440 (4)	2.073	0.209	10.08
CSA S806 (Min. 1-3)	1.206	0.129	10.72
JSCE 97 (6)	1.147	0.135	11.78
El-Ghandour et al. (15)	1.412	0.231	16.39
Matthys and Taerwe (18)	1.251	0.107	8.55
Ospina et al. (19)	0.978	0.083	8.51
El-Gamal et al. (21)	0.870	0.090	10.39
Theodorakopoulos and Swamy (23)	1.096	0.100	9.14
Zaghloul and Razaqpur (20)	0.968	0.104	10.72
IStructE (13)	1.307	0.112	8.55
El-Ghandour et al. (17)	1.045	0.089	8.55

[a] Code provisions for steel-RC slabs only.

equations compared, the analytically derived model of Theodorakopoulos & Swamy (Equation **23**) proved to be the most accurate. It was found that for the 29 slabs analyzed, the mean of the test-to-predicted punching shear strengths was 1.000 ± 0.122 (COV = 12.25%). This model possessed the smallest standard deviation and COV among all the equations tested, in addition to the mean being closest to 1.00. This model considers size effect as well as bond-slip between the GFRP reinforcement and concrete. Additionally, it considers the compressive strength of concrete and flexural reinforcement ratio to be co-dependent entities, not isolated entities as suggested by the other prediction equations.

3.2 Interior Specimens Eccentrically Loaded

These equations were applied to the eccentrically loaded interior slab-column connections tested by Gouda & El-Salakawy (2015). The flexural reinforcement ratio of the connections ranged from 0.65% to 1.30% and the moment-to-shear ratio M/V was constant at 150 mm for all specimens. Table 2 presents the results of each equation by listing their mean V_{TEST}/V_{PRED} value, standard deviation, and COV.

Comparison of the three major code provisions depicts a similar trend as witnessed by the concentrically loaded interior connections. Specifically, the American guideline (Equation **4**) produces highly overestimated predictions with V_{TEST}/V_{PRED} = 1.890 ± 0.115 (COV = 6.07%); whereas the Canadian standard (Equation **1**–Equation **3**) and Japanese standard (Equation **6**) yield slightly overestimated predictions with V_{TEST}/V_{PRED} = 1.005 ± 0.051 (COV = 5.11%) and V_{TEST}/V_{PRED} = 1.126 ± 0.074 (COV = 6.59%), respectively. The standard deviation and COV are significantly lower for the eccentrically loaded interior connections than for the concentrically loaded interior connections, as is expected from a smaller sample size. This must be taken into consideration when comparing the results from each equation as it would be misleading to assume that the code equations yield better results for eccentric loading than concentric loading until further testing has been conducted.

El-Ghandour et al. (Equation **15**), Matthys & Taerwe (Equation **18**), and IStructE (Equation **13**) predict mean V_{TEST}/V_{PRED} values greater than 1.00, as they did for the concentrically loaded specimens. Moreover, the degree of conservatism is approximately the same for both concentrically and eccentrically loaded connections. The remaining equations yield overestimated results by predicting a punching shear strength greater than the observed punching shear strength. The three most accurate equations of the concentric analysis predicted under conservative strengths for the eccentric group. Of the equations, Matthys & Taerwe (Equation **13**) exhibited the most accurate predictions with V_{TEST}/V_{PRED} = 1.049 ± 0.054 (COV = 5.11%).

3.3 Edge Specimens Eccentrically Loaded

The edge specimens of El-Gendy & El-Salakawy (2014) had

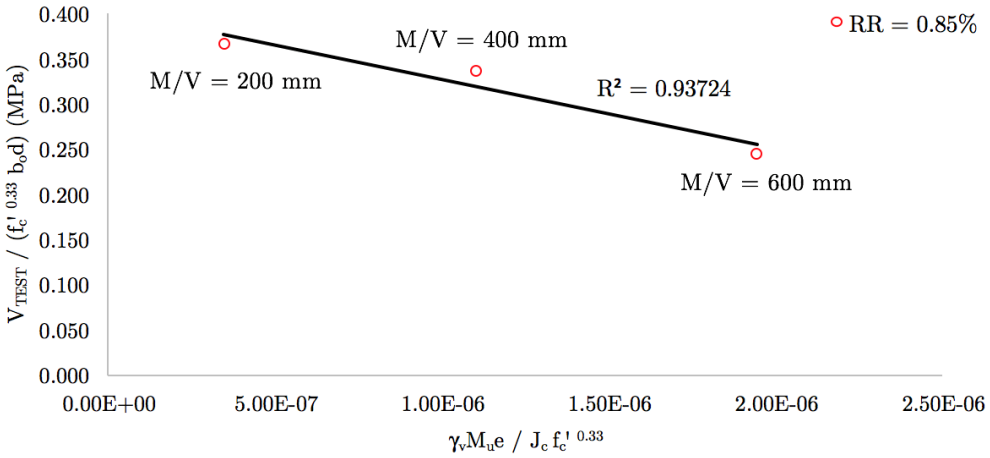

Figure 1: *Effect of moment-to-shear ratio on normalized shear strength.*

flexural reinforcement ratios ranging from 0.85% to 1.70%. Unlike the specimens of Gouda & El-Salakawy (2015), the moment-to-shear ratio M/V varied from 200 mm to 600 mm. Comparison of the previous results with those above shows that many of the proposed prediction equations yielded inconsistent, and in some cases very unsafe, predictions for connections subjected to combined moment and shear transfer. For instance, the most accurate prediction model for concentric loading was found to be that proposed by Theodorakopoulos & Swamy (Equation 23) with V_{TEST}/V_{PRED} = 1.000 ± 0.122 (COV = 12.25%). However, when applied to eccentrically loaded interior (Table 2) and edge (Table 3) columns V_{TEST}/V_{PRED} = 0.917 ± 0.053 (COV = 5.76%) and V_{TEST}/V_{PRED} = 1.096 ± 0.100 (COV = 9.14%), respectively. This suggests that the proposed prediction equations require further modification to be applied safely and reliably to eccentrically loaded slab-column connections.

Three edge specimens were plotted against the unbalanced moment in Figure 1. The coefficient of determination, R^2, was calculated to be 94%. This suggests, therefore, that there is a linear relationship between the moment-to-shear ratio and the normalized punching shear strength. More specifically, the normalized punching shear strength decreases linearly as the moment-to-shear ratio is increased, as assumed by the eccentric shear stress model. This relationship thus validates the assumption of a linear variation in shear stress for flat plates reinforced with GFRP.

4 Conclusion

The following conclusions can be drawn from the comparative study discussed above:

1. CSA S806-12 and JSCE-97 are applicable to GFRP-reinforced connections subjected to eccentric loading;
2. ACI 440-15 highly underestimates the capacity of slab-column connections as it neglects the contribution of the aggregate interlock and dowel action;
3. Many of the proposed equations yield inconsistent, and in some cases unsafe, predictions for interior and edge connections;
4. Results for edge connections support the assumption of a linear stress variation proposed by the eccentric shear stress model;
5. The equivalent steel ratio proposed by El-Ghandour et al. (2000) produced more accurate results than the ratio proposed by the Institute of Structural Engineers, UK (1999).

5 Recommendations for Future Work

Further investigation is warranted to study the effect of the following on the punching shear strength of eccentrically loaded interior, edge and corner connections:

1. Type of reinforcement, including Aramid-, Basalt-, and Carbon-fibre-reinforced polymer, and their respective bond characteristics;
2. Use of HSC;
3. Use of transverse shear reinforcement; and
4. Size effect.

6 Acknowledgements

Firstly, I would like to express my sincerest gratitude to Dr. Ehab El-Salakawy. Throughout my undergraduate degree, Dr. El-Salakawy has shared with me his knowledge and insight regarding the field of reinforced concrete structures and the implementation of GFRP composites as a reinforcing material. It was my privilege to be under his supervision and guidance.

I would also like to acknowledge Mohammed El-Gendy for his continuous support, encouragement, and advice. Mohammed's ability to clearly convey his ideas and expertise in a safe and welcoming environment is what I believe distinguishes him from other academic mentors. He was always happy to offer his help, even if it meant less time for his own work. For that, I am extremely grateful.

References

ACI Committee 318. (1995). *Building code requirements for structural concrete: ACI 318-95.* Detroit, MI, USA: American Concrete Institute.

ACI Committee 318. (2005). *Building code requirements for structural concrete and commentary & PCA notes on 318-05: ACI 318-05.* Detroit, MI, USA: American Concrete Institute.

ACI Committee 318. (2011). *Building code requirements for structural concrete and commentary: ACI 318-11.* Detroit, MI, USA: American Concrete Institute.

ACI Committee 440. (2015). *Guide for the design and construction of structural concrete reinforced with fiber-reinforced polymer bars: ACI 440.1R-15.* Detroit, MI, USA: American Concrete Institute.

British Standards Institution. (1997). *Structural use of concrete - code of practice for design and construction.* London, UK: British Standards Institution.

Canadian Standards Association. (2002). *Design and construction of building components with fibre-reinforced polymers, CAN/CSA 806-02.* Toronto, ON, Canada: Canadian Standards Association.

Canadian Standards Association. (2004). *Design of concrete structures, CAN/CSA A23.3-04.* Toronto, ON, Canada: Canadian Standards Association.

Canadian Standards Association. (2012). *Design and construction of building structures with fibre-reinforced polymer, CAN/CSA S806-12.* Toronto, ON, Canada: Canadian Standards Association.

Dulude, C., Ahmed, E., & Benmokrane, B. (2010). Punching shear strength of concrete flat slabs reinforced with GFRP bars. *2nd International Structures Specialty Conference, Winnipeg, MB, Canada*, 1-9.

El-Gamal, S., El-Salakawy, E. F., & Benmokrane, B. (2005). A new punching shear equation for two-way concrete slabs reinforced with FRP bars. *ACI Special Publication*, *230*, 877-894.

El-Gendy, M., & El-Salakawy, E. F. (2014). Punching shear behaviour of edge slab-column connections reinforced with FRP composite bars. *7th International Conference on FRP Composites in Civil Engineering (CICE 2014), August 20-22, Vancouver, BC, Canada.*

El-Gendy, M., & El-Salakawy, E. F. (2015). GFRP-RC slab-column edge connections with GFRP shear studs. *12th International Symposium on RFP For Reinforced Concrete Structures (FRPRCS-12) & the 5th Asia-Pacific Conference on FRPs in Structures (APFIS-2015) Joint Conference, 14-16 December 2015, Nanjing, China.*

El-Ghandour, A. W., Pilakoutas, K., & Waldron, P. (1999). New approach for punching shear capacity prediction of fiber reinforced polymer reinforced concrete flat slabs. *ACI Special Publication*, *188*, 135-144.

El-Ghandour, A. W., Pilakoutas, K., & Waldron, P. (2000). Punching shear behavior and design of FRP RC slabs. *Proceedings of the International Workshop on Punching Shear Capacity of RC Slabs, Stockholm, Sweden*, 359-366.

El-Ghandour, A. W., Pilakoutas, K., & Waldron, P. (2003). Punching shear behavior of fiber reinforced polymers reinforced concrete flat slabs: Experimental study. *Journal of Composites for Construction*, *7*(3), 258-265.

Gouda, A., & El-Salakawy, E. F. (2015). Finite element modeling on interior slab-column connections reinforced with GFRP bars subjected to moment transfer. *Fibers*, *3*, 411-431.

Gu, X., Jin, X., & Zhou, Y. (2016). *Basic principles of concrete structures.* Berlin, Germany: Springer-Verlag.

Hussein, A., Rashid, I., & Benmokrane, B. (2004). Two-way concrete slabs reinforced with gfrp bars. *4th International Conference on Advanced Composite Material in Bridges and Structures, Calgary, AB, Canada*, 1-8.

IStructE. (1999). *Standard method of detailing structural concrete: A manual for best practice.* London, UK: The Institution of Structural Engineers.

Japan Society of Civil Engineering. (1997). *Recommendation for design and construction of concrete structures using continuous fibre reinforcing materials: Concrete engineering series 23.* Tokyo, Japan: Japan Society of Civil Engineering.

Lee, J. H., Yoon, Y. S., Cook, W. D., & Mitchell, D. (2009). Improving punching shear behavior of glass fiber-reinforced polymer reinforced slabs. *ACI Structural Journal*, *106*(4), 427-434.

Matthys, S., & Taerwe, L. (2009). Concrete slabs reinforced with FRP grids. II: Punching resistance. *Journal of Composites for Construction*, *4*(3), 154-161.

Nguyen-Minh, L., & Rovňák, M. (2013). Punching shear resistance of interior GFRP reinforced slab-column connections. *Journal of Composites for Construction*, *17*(1), 2-13.

Ospina, C. E., Alexander, S. D. B., & Cheng, J. J. R. (2003). Punching of two-way concrete slabs with fiber-reinforced polymer reinforcing bars or grids. *ACI Structural Journal*, *100*(5), 589-298.

Song, J.-K., Kim, J., Song, H.-B., & Song, J.-W. (2012). Effective punching shear and moment capacity of flat plate-column connection with shear reinforcements for lateral loading. *International Journal of Concrete Structures and Materials*, *6*(1), 19-29.

Theodorakopoulos, D. D., & Swamy, N. (2007). Analytical model to predict punching shear strength of FRP-reinforced concrete flat slabs. *ACI Structural Journal*, *104*(3), 257-266.

Theodorakopoulos, D. D., & Swamy, R. N. (2002). Ultimate punching shear strength analysis of slab-column connections. *Cement and Concrete Composites*, *24*, 509-521.

Theodorakopoulos, D. D., & Swamy, R. N. (2008a). A design model for punching shear of FRP-reinforced slab-column connections. *Cement & Concrete Composites*, 544-555.

Theodorakopoulos, D. D., & Swamy, R. N. (2008b). Analytical model to predict punching shear strength of frp-reinforced concrete flat slabs. *ACI Structural Journal*, *104*, S25.

Tureyen, A., & Frosch, R. (2003). Concrete shear strength: Another perspective. *ACI Structural Journal*, *100*(5), 609-615.

Wight, J. K., & MacGregor, J. G. (2011). *Reinforced concrete: Mechanics and design*. Boston, MA, USA: Prentice Hall.

Zaghloul, A., & Razaqpur, A. (2004). Punching shear strength of concrete flat plates reinforced with CFRP grids. *Proceedings of the 4th Conference on Advanced Composite Materials in Bridges and Structures, Calgary, AB, Canada*, 1-8.

2018 Call for Submissions Now Open

ISSN 2561-1127 (Print)
ISSN 2561-1135 (Online)

pmuser@umanitoba.ca
ojs.lib.umanitoba.ca/pmuser